

CHEMOSTRATIGRAPHIC, ALTERATION, AND OXYGEN ISOTOPIC TRENDS IN A PROFILE THROUGH THE STRATIGRAPHIC SEQUENCE HOSTING THE HEATH STEELE B ZONE MASSIVE SULFIDE DEPOSIT, NEW BRUNSWICK

DAVID R. LENTZ¹

*New Brunswick Geological Surveys Branch, P.O. Box 50, 495 Riverside Drive, Bathurst, New Brunswick E2A 3Z1
and Department of Geology, University of New Brunswick, Fredericton, New Brunswick E3B 5A3*

DOUGLAS C. HALL

Electron Microscopy Unit, University of New Brunswick, Fredericton, New Brunswick E3B 6E1

LAWRENCE D. HOY

Tallon Metal Technologies, 1961, rue Cohen, St. Laurent, Québec H4R 2N7

ABSTRACT

This detailed study of a drill hole through the middle Ordovician section that hosts the 25 Mt Heath Steele B zone massive sulfide deposit shows that the local geology has been misinterpreted. Using immobile elements, their ratios, and oxygen isotopes of quartz phenocrysts, distinct stratigraphic footwall (FW) and hanging wall (HW) are recognized in the sedimentary and felsic crystal tuff (CT) sequence; This indicates that the two FW sedimentary packages and FW and HW CT packages do not represent fold repetitions of each other, which has obvious exploration significance. Although extremely transposed, the stockwork and larger alteration system are recognizable with feldspar hydrolysis to phyllosilicates, an increasing proportion of chlorite relative to K mica, and increasing disseminated and vein sulfides toward the ore horizon. These observations are consistent with increasing (>100 m) whole-rock $(\text{Fe} + \text{Mg})/(\text{K} + \text{Na})$ and $\text{Al}_2\text{O}_3/(\text{Al}_2\text{O}_3 + \text{K}_2\text{O} + \text{Na}_2\text{O})$ toward the massive sulfides. In the FW, these trends are coincident with increasing S_T , Cu, Co, As, and Sb, reflecting sulfide saturation. The HW alteration is <50 m wide and manifested by slightly higher $(\text{Fe} + \text{Mg})/(\text{K} + \text{Na})$, Eu/Eu*, Fe, Mn, Mg, S, Ba, Co, Cu, Zn, Pb, Sb, and Hg than rocks further up in sequence. The mineralogy and mineral compositions reflect upper greenschist grade (450°C and 600 MPa) conditions with an overall equilibrium distribution of major and trace elements. In the least-altered FW CT, chessboard albite variably replaces alkali feldspar phenocrysts and, with increasing alteration, are hydrolyzed to micas. The Fe/(Fe + Mg) and Al contents of K-mica (phengite – muscovite) and chlorite (ferroan clinocllore to chamosite) increase, reflecting alkali-element leaching, variable silica leaching, and Fe and Mg exchange reactions at low pH and high Fe/Mg in the fluid. In the HW, hydrolysis of feldspar to Ba-bearing phengite and Fe clinocllore is indicative of continued fluid venting through the CT and mixing with shallowly circulating seawater. At an estimated temperature of 400°C, stockwork chlorite compositions ($X_{\text{chamosite}} = 0.8$) indicate an $\text{Fe}/\text{Mg}_{\text{fluid}} = 200$ for the buoyant mineralizing hydrothermal plume, whereas the distal chlorite alteration ($X_{\text{chamosite}} = 0.3$) reflects local seawater-dominated alteration peripheral to the mineralizing plume. Whole-rock $\delta^{18}\text{O}$ values, closely reflecting chlorite content, decrease toward the ore horizon to 5.3‰ (FW chloritite). At inferred temperatures between 300 and 400°C, the ore-forming fluid has a high ^{18}O content (≈ 5 to 7‰) indicative of extensively modified seawater, typical of those forming large VMS deposits. In the HW, whole-rock $\delta^{18}\text{O}$ values decrease toward the ore horizon from >11‰ to 8.7‰ in the altered rock.

Keywords: massive sulfide, VMS deposit, litho geochemistry, chemostratigraphy, hydrothermal alteration, oxygen isotopes, Heath Steele, Bathurst Camp, New Brunswick.

SOMMAIRE

D'après les résultats d'une étude détaillée de carottes de sondage traversant la séquence ordovicienne moyenne qui contient le gisement de sulfures massifs de Heath Steele, zone B (25 Mt), le contexte géologique aurait été mal interprété. Nous avons utilisé les teneurs en éléments immobiles, les rapports de celles-ci, et le rapport des isotopes d'oxygène dans le quartz phénocristique pour reconnaître les roches stratigraphiquement sous-jacentes et sus-jacentes dans la séquence de métasédiments et de tufs felsiques enrichis en cristaux. Nous ne croyons pas que les deux séquences sédimentaires sous-jacentes et les séquences de tufs à cristaux fragmentés sous-jacente et sus-jacente (par rapport à la zone minéralisée) représentent des unités répétées par plissement; cette interprétation a une signification importante dans les modèles d'exploration. Quoique la transposition d'unités peut être extrême, le stockwerk et le système d'altération plus étendu sont reconnaissables grâce à l'hydrolyse du feldspath, pour donner des

¹ E-mail address: dlentz@gov.nb.ca

phyllosilicates, une augmentation dans la proportion de chlorite par rapport au mica blanc, et une augmentation dans la proportion de sulfures disséminés et en veines vers l'horizon minéralisé. Ces observations rendent compte de l'augmentation, sur plus de 100 m, des valeurs $(Fe + Mg)/(K + Na)$ et $Al_2O_3/(Al_2O_3 + K_2O + Na_2O)$ dans les roches globales en direction de l'horizon minéralisé. Dans les roches sous-jacentes à cet horizon, ces tendances progressent avec une augmentation en S total, Cu, Co, As et Sb, qui indique la saturation du système en sulfures. Dans les roches sous-jacentes, l'enveloppe d'altération, inférieure à 50 m, se manifeste par un rapport $(Fe + Mg)/(K + Na)$ et Eu/Eu^* plus élevé, et des teneurs en Fe, Mn, Mg, S, Ba, Co, Cu, Zn, Pb, Sb et Hg légèrement plus élevées, que plus haut dans la séquence. Les assemblages de minéraux et leur composition concordent avec des conditions dans le faciès schiste vert supérieur (450°C, 600 MPa), et semblent indiquer l'équilibre dans la distribution des éléments majeurs et des éléments traces. Dans les tufs à cristaux inférieurs les moins altérés, l'albite à texture en damier remplace les phénocristaux de feldspath alcalin à un degré variable et, avec augmentation du degré d'altération, se voit transformé en micas. Le rapport $Fe/(Fe + Mg)$ et la teneur en Al du mica blanc (muscovite phengitique) et de la chlorite (clinocllore ferreuse à chamosite) augmentent, suite au lessivage des alcalins et de la silice, et aux réactions d'échange impliquant Fe et Mg à faible pH et rapport Fe/Mg élevé. Dans les roches sous-jacentes, l'hydrolyse du feldspath pour donner une phengite baryfère et une clinocllore ferreuse semble indiquer le flux soutenu d'une phase fluide à travers des tufs à cristaux et un mélange avec de l'eau de mer mis en circulation à faible profondeur. A une température de 400°C, la composition de la chlorite du stockwerk ($X_{chamosite} = 0.8$) indique une valeur Fe/Mg dans le fluide de l'évent d'environ 200, tandis que la composition de la chlorite des zones distales d'altération ($X_{chamosite} = 0.3$) semble plutôt régie par l'eau de mer. Les valeurs de $\delta^{18}O$ des roches globales, qui dépendent directement du contenu en chlorite, diminuent jusqu'à 5.3‰ (chlorite sous-jacente) dans la direction de la zone minéralisée. A une température probable entre 300 et 400°C, la phase fluide responsable de la minéralisation aurait eu une teneur élevée en ^{18}O (entre 5 et 7‰), et donc aurait été une saumure fortement modifiée, telle que dans le cas des gisements de sulfures volcanogéniques massifs plus importants. Les valeurs $\delta^{18}O$ des roches sous-jacentes altérées diminuent de >11‰ à 8.7‰ dans la direction de la zone minéralisée.

(Traduit par la Rédaction)

Mots-clés: sulfures massifs, gisement de type VMS, lithogéochimie, chemostratigraphie, altération hydrothermale, isotopes d'oxygène, Heath Steele, camp minier de Bathurst, Nouveau-Brunswick.

INTRODUCTION

Heath Steele, the second largest Zn–Pb–Cu–Ag massive sulfide deposit in the Bathurst Mining Camp, is located about 65 km southwest of Bathurst, in northern New Brunswick (Fig. 1). The Heath Steele B Zone, the largest deposit known in the Heath Steele belt, has produced 17.9 Mt grading 1.73% Pb, 4.67% Zn, 0.96% Cu, and 63 g/t Ag, mined intermittently between 1957 and 1997. As of 1993, ore reserves at the B Zone totalled 3 Mt at grades similar to historical values (McCutcheon 1992, Hamilton *et al.* 1993).

The massive sulfide deposits (A to E, Fig. 1) within the Heath Steele belt are hosted by crystal-rich felsic volcanoclastic rocks and associated tuffaceous sedimentary rocks of the Nepisiguit Falls Formation, which forms the basal part of the Middle Ordovician Tetagouche Group (Skinner 1974, van Staal & Fyffe 1991, Wilson 1993). The enclosing host rocks and the sulfide deposits are highly deformed (McBride 1976), with at least four phases of deformation (Moreton & Williams 1986, de Roo *et al.* 1990, 1991, 1992, Moreton 1994), and are metamorphosed from lower to upper greenschist grade.

This whole-rock geochemical, mineral-chemical, and oxygen isotopic study of the B zone deposit (Fig. 2) was undertaken: 1) to investigate the relationship between the hanging-wall (HW) quartz-crystal-rich tuff (QCT), which occurs immediately above the massive sulfides and coeval iron-formation, and the quartz-feldspar crystal-rich tuff (QFCT) that occurs 50 to 100 m higher in the stratigraphy, 2) to describe the alteration systematics in the HW and footwall (FW), 3) to link the mineral-chemical variations with the whole-rock geochemical variations,

and 4) to compare the HW CT to a similar rock type that occurs in the structural FW, as the latter has recently been inferred to be a structural repetition of the former (de Roo *et al.* 1991, Moreton 1994). In addition, all units were characterized chemically in order to help correlate units chemostratigraphically among the various massive sulfide deposits. With these objectives in mind, a recent underground exploration diamond-drill-hole (DDH HSB3409) that transected much of the mine sequence was selected for detailed analysis. The hole was collared (Fig. 3) in the stratigraphic FW and drilled northward into the HW CT in order to test for fold repetitions of the ore horizon.

The detailed results of this chemostratigraphic analysis conflict with structural interpretations of the Heath Steele B zone area (de Roo *et al.* 1991, Moreton 1994). Therefore, the local mine stratigraphy is presented in revised form, and uses recognized subdivisions and nomenclature of the Bathurst Mining Camp (van Staal & Fyffe 1991).

REGIONAL GEOLOGICAL SETTING

The stratigraphy around Heath Steele Mines consists of intercalated quartz wackes and carbonaceous pelites that resemble the Miramichi Group (Fig. 1). However, the rocks locally contain fine-grained CT horizons and, therefore, by definition, are included in the Nepisiguit Falls Formation of the Tetagouche Group. In the Heath Steele area, the Tetagouche Group has been subdivided into two parts, a lower part comprising volcanic, volcanoclastic, and sedimentary rocks (Nepisiguit Falls Formation, Fig. 4), and an upper part consisting of rhyolite and hyaloclastic tuff (Flat Landing Brook

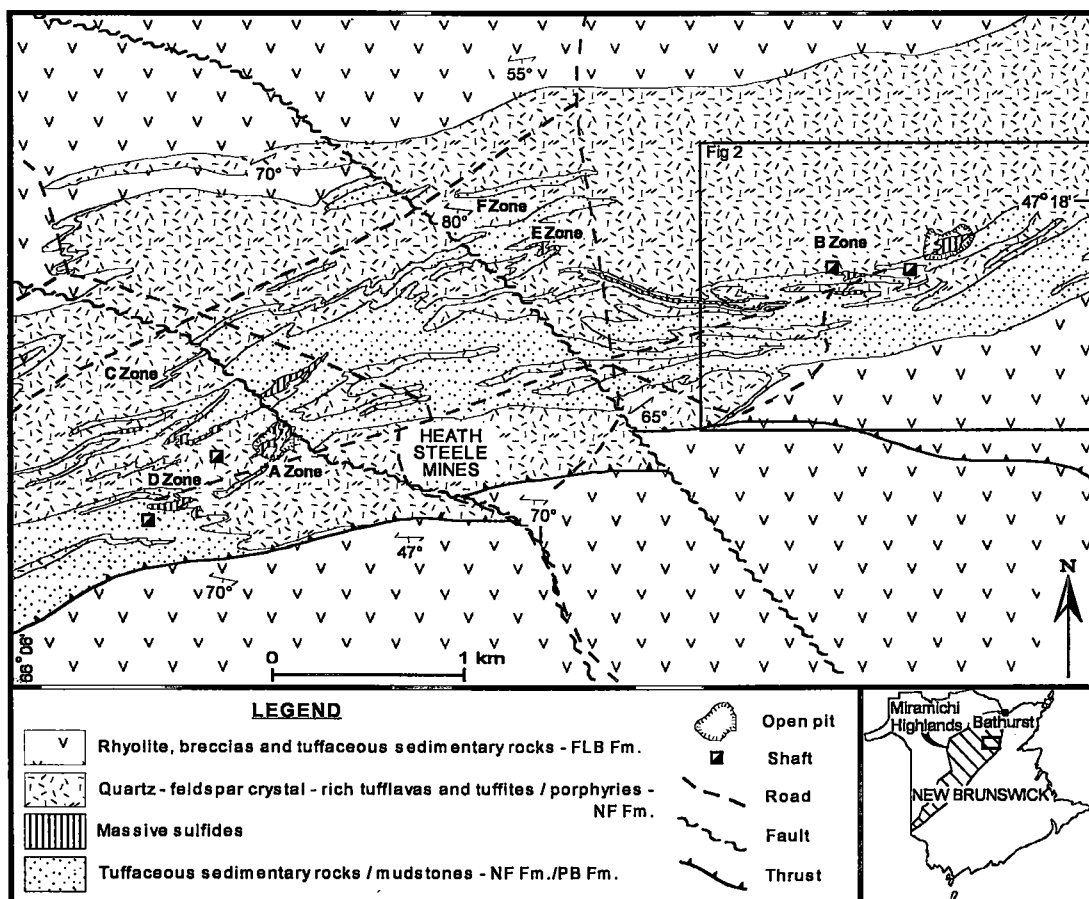


FIG. 1. Location of the Heath Steele A, B, C, D, E, and F zones and Stratmat massive sulfide deposits (after Hamilton *et al.* 1993).

Formation, Fig. 4; van Staal & Fyffe 1991, van Staal *et al.* 1992, Wilson 1993). Unlike the Brunswick No. 6 and 12 deposits to the northeast, the Heath Steele massive sulfide deposits and associated iron-formation occur within the Nepisiguit Falls Formation (McCutcheon *et al.* 1993).

Intense deformation and metamorphism began during the Late Ordovician (Ashgillian) with D₁ thrusting and tight folding, but continued into the Devonian with the culmination of the Acadian Orogeny (van Staal & Fyffe 1991, van Staal *et al.* 1992). At least five generations of folds have been identified in the Bathurst Mining Camp (van Staal 1987, de Roo *et al.* 1990, 1991).

LOCAL SETTING

The rocks of the Heath Steele belt are, in part, bounded to the north and south by a sequence of massive rhyolite and coarse pyroclastic rocks (lapilli tuff, breccia and agglomerate) of the Flat Landing Brook Formation, which are locally in fault contact to the south (Heath Steele fault, Fig. 2, Wilson 1993). This structure was first described as a broad antiformal fold by Dechow (1960), although

de Roo *et al.* (1990) and Moreton (1994) suggested that the entire sequence is in thrust contact with the rhyolites to the south. The position of the iron-formation and the styles of alteration (McMillian 1969, Whitehead 1973, McBride 1976, Owsiaki 1980) imply that the sequence is north-younging at the B zone deposit.

MINE STRATIGRAPHY

The mine stratigraphy has been described in detail by McBride (1976) and Moreton & Williams (1986), but was revised on the basis of structural observations by de Roo *et al.* (1991) and Moreton (1994) (Fig. 4). McBride (1976) suggested that a horizon of CT occurs in the stratigraphic footwall, whereas de Roo *et al.* (1991) suggested that it represents infolded hanging-wall, an interpretation that has major implications for possible repetition of the mineralized horizon. In contrast to the model of de Roo *et al.* (1991), the geochemical evidence presented later closely resembles McBride's (1976) earlier stratigraphic interpretation; therefore, a revised stratigraphic column is proposed (Fig. 4). The detailed geology in Figure 2

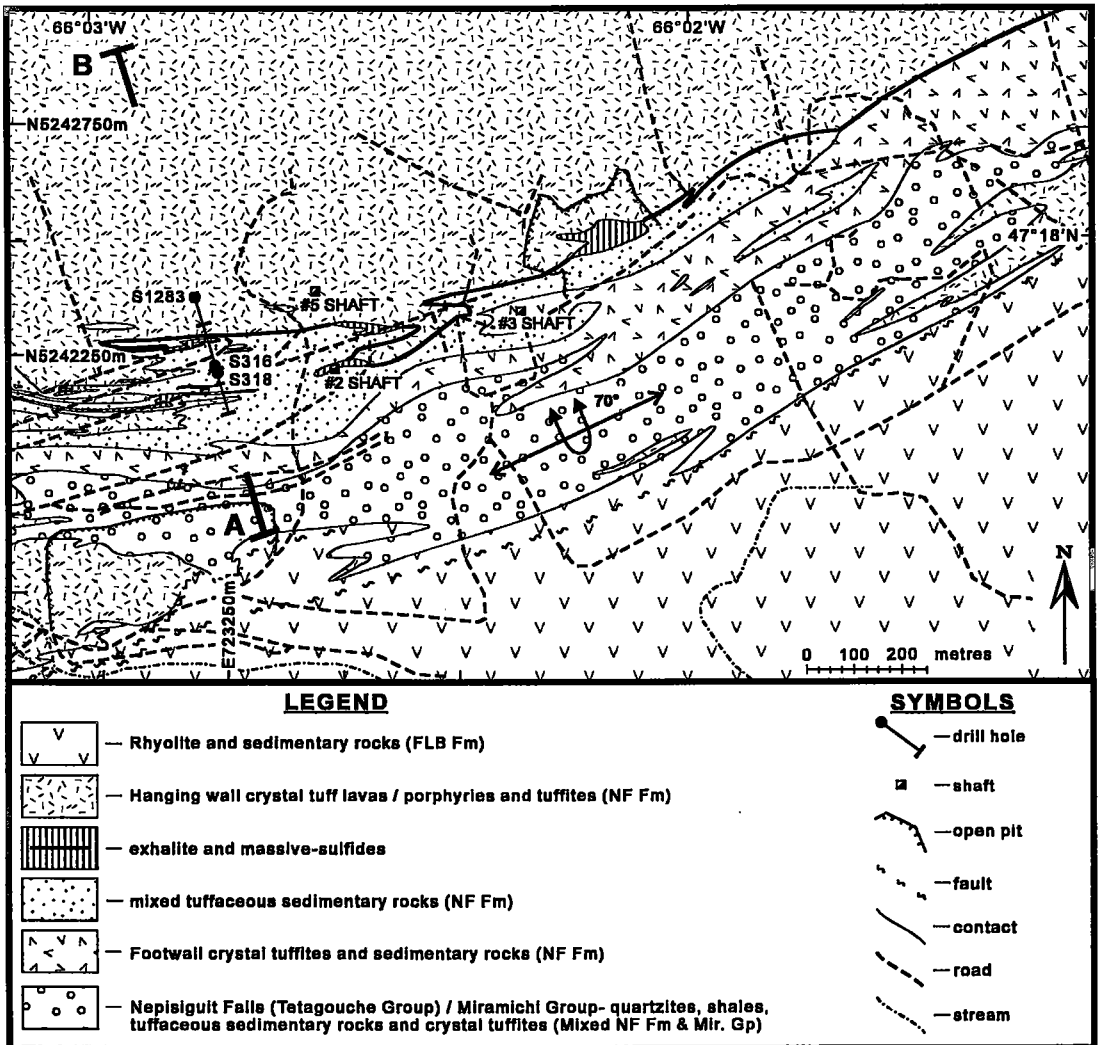


FIG. 2. Geological map of the Heath Steele B-zone orebodies (after Lentz & Wilson 1997), with the location of the A-B cross section illustrated in Figure 3. Abbreviations: FLB: Flat Landing Brook Formation (Tetagouche Group), NF: Nepisiguit Falls Formation (Tetagouche Group), Mir. Gp: Miramichi Group.

reflects these revisions, based on further chemostratigraphic work in the area (Lentz & Wilson 1997).

Lower footwall (FW) sedimentary package

McBride (1976) described a sequence of locally graphitic, interlayered mudstones and quartzose siltstones and sandstones (Fig. 5) in the lower stratigraphic footwall to the B zone deposit. Overall, this unit resembles rocks of the Miramichi Group (see van Staal & Fyffe 1991, Langton & McCutcheon 1993) that typically underlie felsic CT and related sedimentary rocks of the Nepisiguit Falls Formation, although a few occurrences of CT within it indicate that it belongs in the Tetagouche Group.

Footwall crystal-rich tuff (FW CT)

This unit contains 15 to 30 vol.% reworked crystals dominated by quartz, but locally also with feldspar (relict microcline and albite) (Fig. 6). As recognized by McBride (1976), this unit locally comes in contact with the ore zone; the upper FW sedimentary package forms sub-basins on either side of the CT. This depositional relationship, evident in mine plans and sections, implies that this is not the same CT that occurs in the stratigraphic and structural HW. A volcanic origin for this unit is supported by the occurrence of vitreous quartz paramorphs after β -quartz phenocrysts, embayed phenocrysts, and broken crystals, the position of this porphyritic unit between two

different sedimentary units, and the occurrence of volcanoclastic material in the overlying (upper FW) sedimentary rocks.

Upper footwall (FW) sedimentary package

This unit is composed of relatively homogeneous mudstones (now phyllites and fine-grained schists) and local volcanoclastic layers with quartz crystals (phenocrysts), and resembles the characteristic Nepisiguit Falls rocks (Wilson 1993). The intensity of the green coloration increases toward the massive sulfide body, which represents an increasing proportion of chlorite that is coincidentally becoming more Fe-rich. These tuffaceous sedimentary rocks form the immediate footwall sequence to the massive sulfide deposits and host minor chalcopyrite – sphalerite – pyrrhotite – pyrite stringer veins in a dark green chloritic groundmass (Fig. 7). A leucocratic unit, which underlies the ore lenses, is described as acid tuff (McBride 1976, Wahl 1978, Moreton & Williams 1986, Moreton 1994); however, it represents sulfidic Mg-rich footwall sedimentary rocks that underwent secondary alteration processes of variable intensity.

Massive sulfides

The massive sulfides and intervening exhalative sedimentary rocks (iron-formation) are generally coeval among all the known deposits in the Heath Steele area. The massive sulfides were described in detail by Lusk (1969, 1992) and Chen & Petruk (1980). The B Zone deposit has three dominant ore-types, massive pyrite, banded pyrite – sphalerite – galena, and pyrrhotite – chalcopyrite fragmental ore with, overall, Cu, Co, and As contents higher and Zn, Pb, and Ag lower than in the Brunswick No. 12 deposit (Hamilton *et al.* 1993). The Heath Steele B Zone deposit is discontinuously overlain by iron-formation (McMillian 1969) that is mineralogically very similar to that between the Brunswick No. 6 and 12 deposits. Lusk (1969, 1992) outlined a pattern of base-metal zoning from the stratigraphic footwall to the hanging wall of the B Zone deposit, and also noted two Cu-rich basal zones associated with the thickest “porphyry” beneath the footwall sedimentary rocks. However, de Roo *et al.* (1991, 1992) refuted the interpretation of the base-metal zoning because of the tight F_1 folding within the sulfide layer (see also Moreton 1994) and the high concentrations of chalcopyrite in the D_1 structurally remobilized sulfide breccia (McDonald 1984).

Hanging-wall crystal-rich tuff (HW CT)

Overlying the massive sulfides and associated banded iron-formation is a horizon of QCT that is concordant to layering and that passes vertically into QFCT (Nepisiguit Falls Formation) away from the deposit. The quartz and K-feldspar crystals comprise 15 to 25 vol. % of the rock,

although within 50 m of the ore horizon, the feldspar crystals disappear over a 5 m vertical interval (Fig. 8). The size of the feldspar crystals decreases from 5 mm to <1 mm in this interval, but this may be an alteration-induced phenomenon. Within the zone of alteration stratigraphically above the ore, pyrite is present, but usually in amounts less than a few modal percent. Siderite also is present in this zone, but locally occurs elsewhere in the hanging wall.

STRUCTURE

McBride (1976) and Moreton (1994) have defined at least five deformation events in detailed structural analyses of the B zone deposit. McBride (1976) suggested that the S_1 foliation associated with isoclinal folds contains a steep, west-plunging lineation (L_1) that was folded around the F_2 folds. Moreton (1994) found that the tight to isoclinal recumbent folds (F_1) have sheath-like profiles and probably formed in a high-strain fold-and-thrust environment. In contrast to McBride (1976), Moreton (1994) suggested that the vergence of the F_1 folds is toward the southeast.

F_2 folds are open to tight folds of the earlier layering, with moderate westerly plunge and a moderate (45°) south-dipping axial-planar foliation. The S_2 foliation generally obliterates the S_1 cleavage through transposition. In general, the enveloping surface to the F_2 folds defines the tabular nature of the sulfide deposit, which lies on the short limb of an overturned F_2 fold.

Post- F_2 deformation events are characterized by open folds of the main S_1S_2 composite foliation. Horizontal folds with flat to shallowly dipping axial surfaces (F_3 or F_4 ; de Roo *et al.* 1990, 1991) define the third event of deformation and cause the local variability in the dip of S_2 .

LITHOGEOCHEMISTRY

Chemostratigraphic interpretation

In order to ascertain the geochemical variations around the deposit, the raw data for hole HSB3409 (available at the Depository of Unpublished Data, CISTI, National Research Council, Ottawa, Ontario K1A 0S2) were plotted as a function of depth using different symbols for the major lithological units (Figs. 9a, b). Table 1 presents the average composition and standard deviation of each of the recognized units, including samples that are considerably altered. Only relatively immobile elements were used to identify compositional differences in the lithologic sequence. In general, Al, Ga, Ti, Sc, Zr, Hf, heavy rare-earth elements (HREE), Y, Th, and Nb are considered to be relatively immobile in the weathering environment (Taylor & McLennan 1985) and are, therefore, useful for petrogenetic studies of sedimentary rocks. In altered and metamorphosed volcanic rocks, these same elements are generally found to be relatively immobile

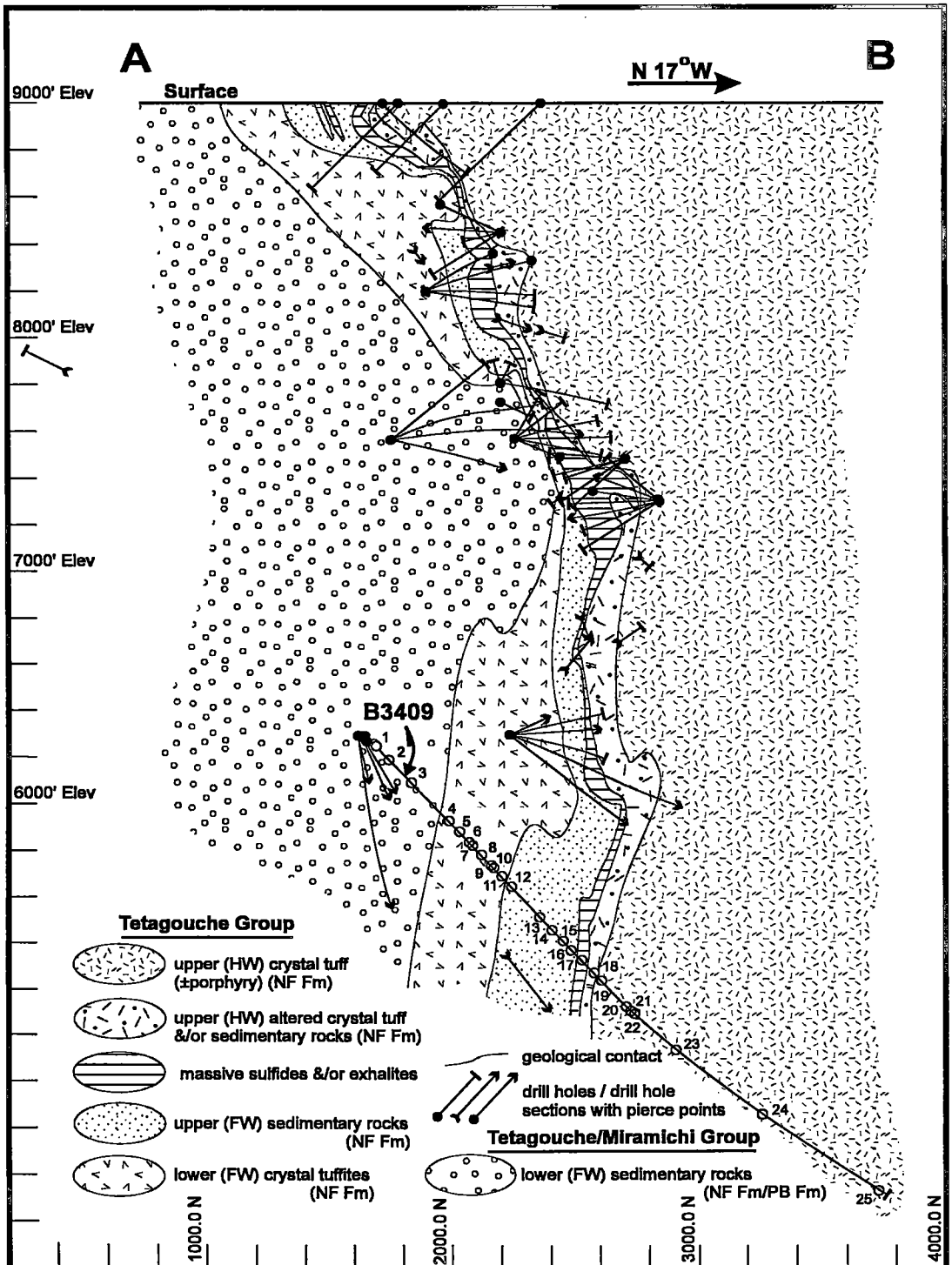


FIG. 3. Geological cross-section through the B-zone deposit illustrating the location of diamond drill-hole (DDH) HSB3409. Abbreviations: HW: hanging wall, FW: footwall, NF: Nepsiguit Falls Formation (Tetagouche Group), PB: Patrick Brook Formation (Miramichi Group).

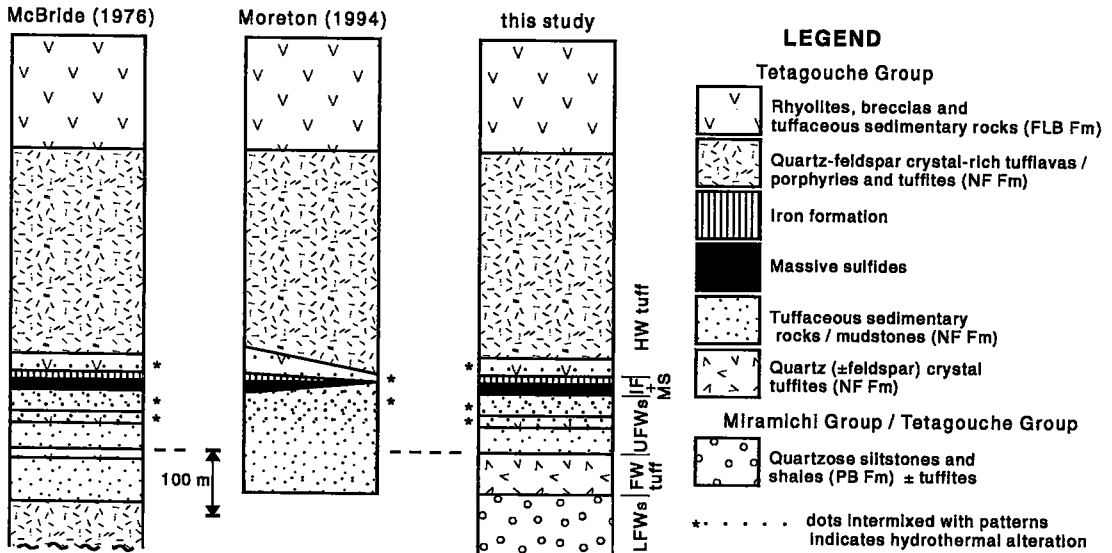


FIG. 4. Schematic stratigraphic columns of the Heath Steele area showing the two previous interpretations of the mine stratigraphy (McBride 1976, Moreton & Williams 1986, de Roo *et al.* 1991, Moreton 1994) compared with that proposed in this study. Lsed: lower FW sedimentary rock, FW CT: FW crystal tuff, Used: upper FW sedimentary rock, HW CT: hanging-wall crystal tuff, NF Fm: Nepisiguit Falls Formation, FLB Fm: Flat Landing Brook Formation.

(Davies *et al.* 1979, Davies & Whitehead 1980, Dostal & Strong 1983, Lentz & Goodfellow 1993a, MacLean & Barrett 1993, Lentz 1996a, b).

As shown in Figure 10, the Ti contents in the lower sedimentary package (0.9 to 1.1 wt.% TiO₂) are distinct from the upper footwall sedimentary package (0.4 to 0.7 wt.% TiO₂). Al contents are also greater in the lower (>15 wt.% Al₂O₃) compared to the upper (<15 wt.% Al₂O₃) sedimentary package. The relatively high contents of Al and Ti in the lower sedimentary section resemble those of the quartzose siltstone and slates of the Miramichi Group (Lentz *et al.* 1996), although the presence of minor intercalated, fine-grained CT horizons by definition indicates that it is part of the Nepisiguit Falls Formation (Wilson 1993). The variation in Ti and Al contents of the upper sedimentary unit relative to the lower sedimentary unit and the footwall CT (Fig. 10) indicates continued pelagic sedimentation during deposition of the tuffaceous (upper) sedimentary rocks, particularly at the top of the sedimentary section. Like TiO₂, Cr, Sc, and V contents (Fig. 11) are also much higher in the lower sedimentary sequence, although they increase upward near the top of the unit, where the most intensely altered rocks occur. The high Cr, Ni, and V, as well as other immobile elements (*i.e.*, Ti, Sc, Al, Zr), at the top of the upper sedimentary sequence indicates an increase in pelagic Miramichi Group sedimentation and a decreased input of tuff just before the massive sulfide was deposited.

The overall difference in composition between the footwall sedimentary packages indicates that they have different provenances. The composition of the lower sedimentary sequence is very similar to quartzose rocks of the Miramichi Group at the FAB zone between Brunswick No. 6 and 12 deposits (Lentz & Goodfellow 1994a), at Key Anacon (Lentz 1995b), and at Middle River, located north of the Brunswick No. 12 deposit (Lentz *et al.* 1996). The upper sequence is compositionally similar to tuffaceous sedimentary rocks of the Nepisiguit Falls Formation (Langton & McCutcheon 1993, Wilson 1993, Lentz & Goodfellow 1996). However, the upper package of sedimentary rocks also is chemically distinct (*i.e.*, higher TiO₂, Sc, Zr, Cr) from the lower footwall CT, indicative of a different felsic volcanic or mixed tuff–pelite source.

There are important chemical differences between the footwall and hanging wall, particularly in their levels of incompatible high-field-strength elements (Y, HREE, Th, and Zr). Overall, the SiO₂ (>70 wt.%) and alkali elements (6 to 7 wt.% K₂O + Na₂O) indicate a rhyolite composition (Le Bas *et al.* 1986). However, they fall in the rhyodacite compositional field of the Winchester & Floyd (1977) (Fig. 12a), similar to the CT between Brunswick and Heath Steele (Lentz & Goodfellow 1992a, b, Langton & McCutcheon 1993, Wilson 1993, Lentz 1996a). The higher Zr and lower TiO₂ in the hanging-wall CT sequence compared to the FW sequence (Fig. 12a) reflects increased chemical evolution of the HW CT.

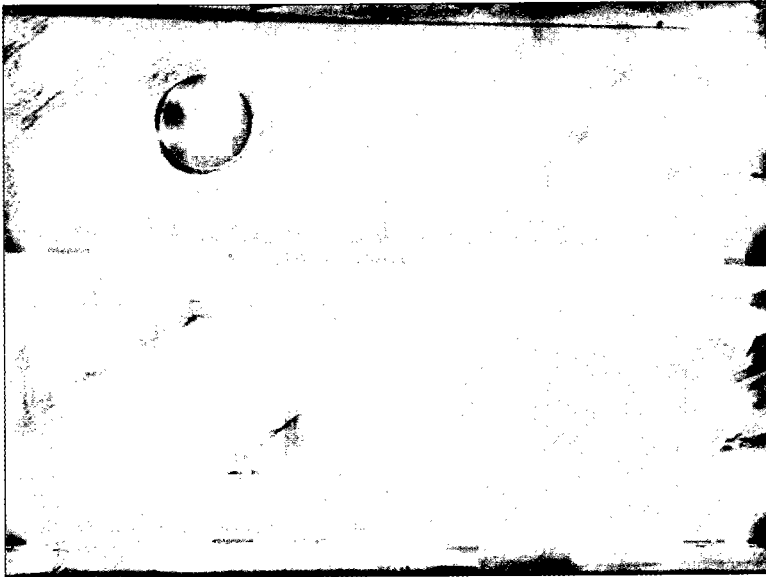


FIG. 5. Quartzose siltstone with interlayered graphitic pelite folded by F_1 (very tight) and F_2 (tight to open). This unit (lower FW sedimentary package) is most similar to the Miramichi Group. These sedimentary rocks represent the upper part of the Miramichi Group sequence (van Staal & Fyffe 1991) (DDH HSB3409, 100.6 m).

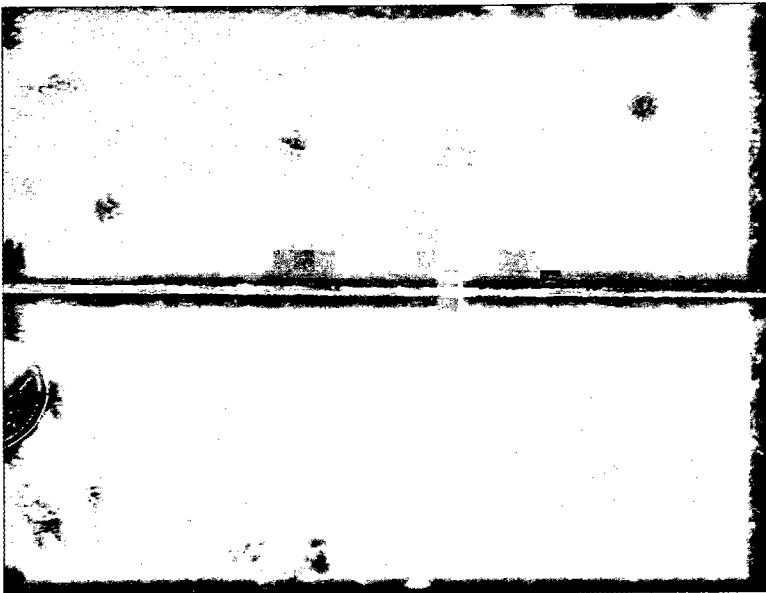


FIG. 6. Light green, fine- to medium-grained, FW CT with vitreous high-temperature quartz phenocrysts and whitish (milky) quartz \pm mica \pm feldspar (relict feldspar phenocrysts) (DDH HSB3409, 230 m).



FIG. 7. Dark green (chloritic), texturally homogeneous FW sedimentary rocks (upper FW sedimentary package) with chalcopyrite – pyrrhotite – pyrite sulfide layers and veins located at the base of the massive sulfide. Folding of the sulfide veins and layers is evident (DDH HSB3409, 400 m).



FIG. 8. Patchy chloritic alteration in the transition zone between the altered QCT and QFCT in the HW (DDH HSB3409, 459.4 m).

The Nb/Y ratio of less than 0.8 is indicative of a subalkaline composition (Figs. 12a, b), consistent with the low Zr contents (100 to 250 ppm) in both tuff units (see Leat *et al.* 1986). The Nb + Y contents indicate that these felsic magmas are transitional between volcanic arc and within-plate compositional fields (Figs. 12c, d; Pearce *et al.* 1984), typical of intracontinental backarc environments (Lentz 1996a). The low Ga/Al value (on average 2.3), derived from Wilson (1993), is inconsistent with an anorogenic origin (Whalen *et al.* 1987). The Y and Zr contents in the hanging-wall CT (on average 43 ppm and 146 ppm, respectively) are slightly higher than the footwall CT (on average 35 ppm and 130 ppm, respectively) (Fig. 13a) and plot in the "tholeiitic" rhyolite field that is normally associated with bimodal magmatism.

The footwall CT has less than 140 ppm Zr, and the hanging-wall unit has greater than this amount (Fig. 13b). Thorium contents are also different (FW CT: 9 to 11 ppm Th, HW CT: 13 to 14 ppm Th). The LREE and HREE contents are slightly higher in the HW CT than in the FW CT (Figs. 13c, 14). The La_N/Lu_N of the hanging-wall CT (on average 6.4) is higher than that of the FW tuff (on average 5.7).

Overall, the distinct compositions of the hanging-wall and footwall tuffs imply that they do not represent the same CT units; this inference contrasts with the structural interpretations of de Roo *et al.* (1990, 1991) and Moreton (1994).

Alteration

At the Brunswick No. 12 deposit, a primary halo of alteration and stringer-sulfide stockwork zone have been recognized (Goodfellow 1975, Juras 1981, Luff *et al.* 1992, Lentz & Goodfellow 1993a, b, c, 1994b, 1996); these are predeformational in origin (Luff *et al.* 1992, Lentz & van Staal 1995). Major-element and base-metal compositional changes have been studied around the Heath Steele deposits by Whitehead (1973), Whitehead & Govett (1974), Goodfellow & Wahl (1976), and Wahl (1978).

In this study, a numerical designation of the alteration zones was used (Alteration Index, Fig. 9b) to help map alteration at Heath Steele; that designation was originally developed in the Brunswick No. 12 study (Lentz & Goodfellow 1994b). It is based on the presence or absence of feldspar, intensity of green coloration, presence of stockwork sulfides, and degree of silicification, with a transition from least-altered type (distal zone 5) to most-altered type (proximal zone 1), typically a silicified sulfide stockwork zone. QFCT and sedimentary rocks in the structural footwall of the Heath Steele massive sulfide deposits are altered within the vicinity (>100 m) of the deposits. Alkali feldspar is altered to a chlorite-sericite assemblage, although albite is still locally preserved (Wahl 1978). Some of the most intense alteration in the area is associated with the orebodies of the C zone (Wahl 1978).

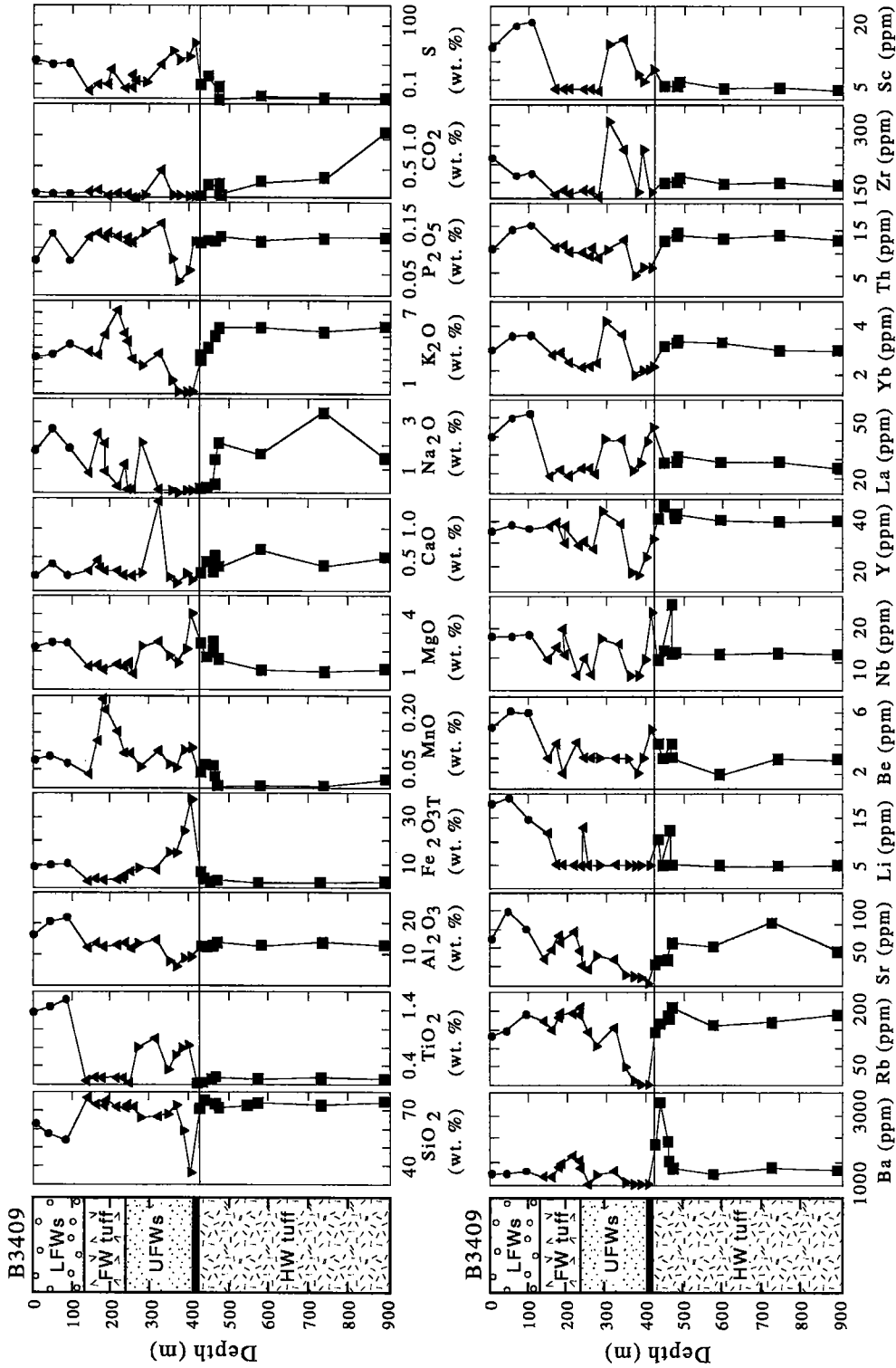


Fig. 9a. Whole-rock geochemical profiles illustrating major- and trace-element compositions for samples from DDH HSB3409 (data file has been deposited, and is available from CISTL, see text). Symbols: lower sedimentary rocks (Lsed, ●), FW crystal tuff (FW CT, ▲), upper sedimentary rocks (U sed, ▼), and hanging-wall crystal tuff (HW CT, ■).

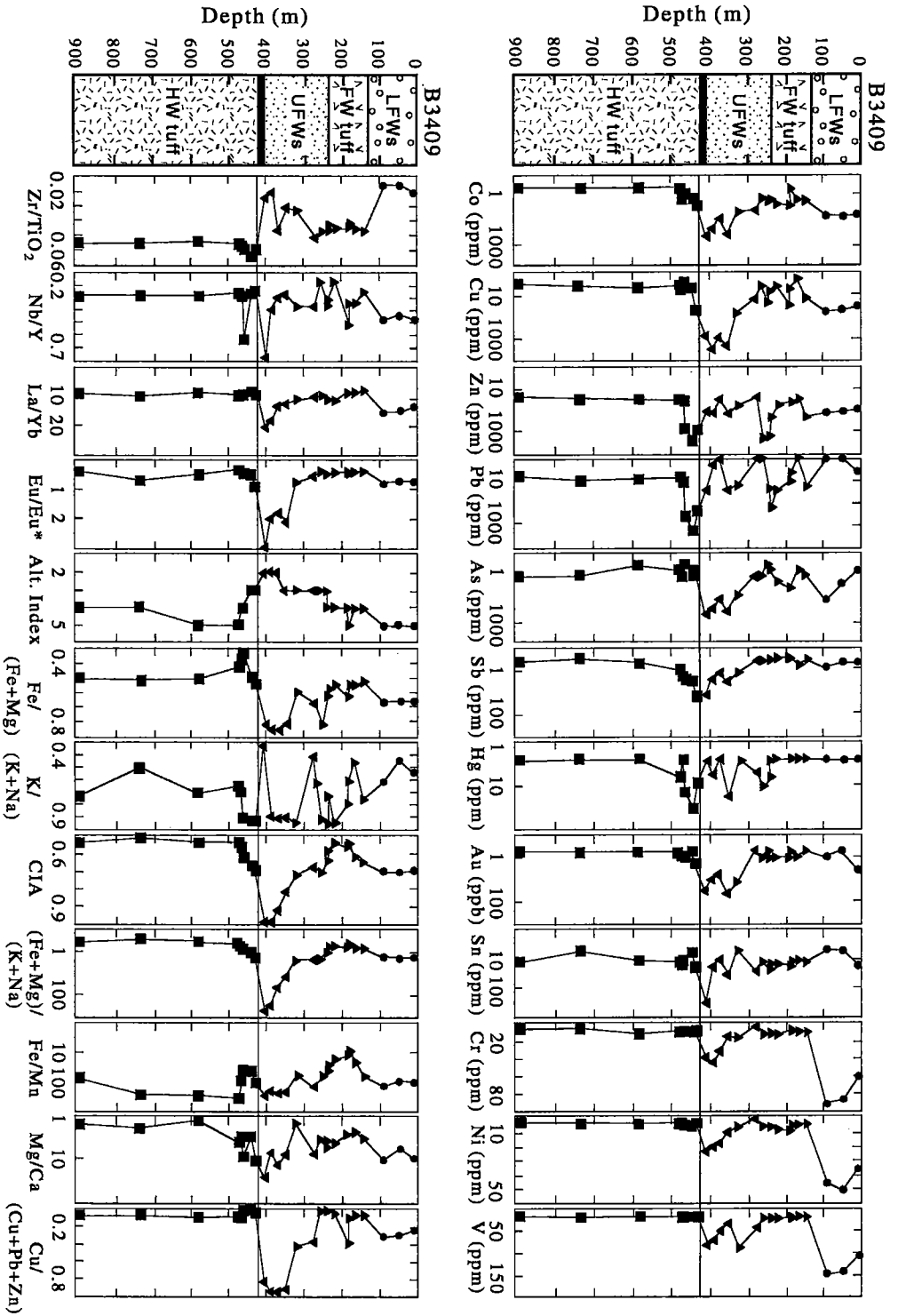


FIG. 9b. Whole-rock geochemical profiles illustrating trace-element compositions and immobile-element ratios and alteration indices for samples from diamond drill-hole HSB3409. Symbols as in Figure 9a.

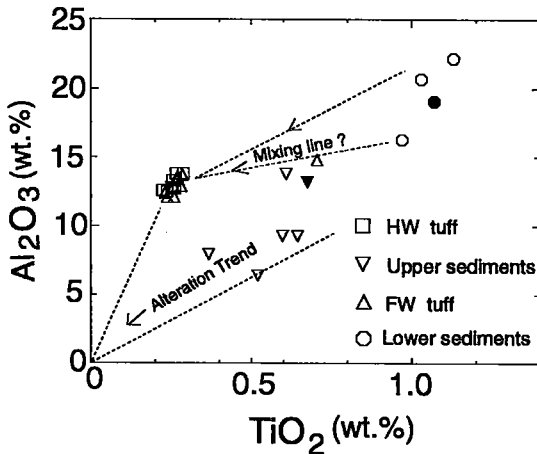


FIG. 10. TiO_2 versus Al_2O_3 contents of samples from DDH HSB3409 (open symbols), as well as two bulk samples of the lower and upper sedimentary rock packages (solid symbols). A hypothetical mixing line between FW volcanoclastic rocks and the lower sedimentary package may give rise to the compositional spectrum of the upper FW sedimentary package inferred to be tuffaceous in origin. The alteration trend depicts the dilution of immobile components due to mass addition to the rock.

Using discriminant analysis, Whitehead & Govett (1974) found that Pb contents are higher (>30 ppm) in the hanging-wall rocks above the B zone deposit. Whitehead (1973) also found that the Mn/Fe value is relatively low in the footwall of the ore zone, but higher in the iron-formation and in the hanging-wall rocks that both overlie the deposits and are also distal with respect to the sulfides. Wahl (1978) showed that Fe, K and Mg are enriched in the footwall porphyry and sedimentary rocks of the B zone deposit, with Na and Ca depleted in

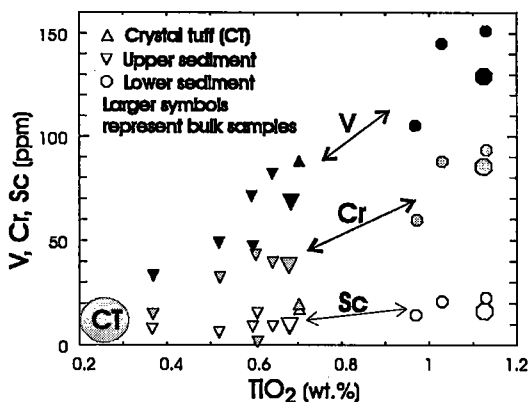


FIG. 11. TiO_2 versus V, Cr, and Sc variation diagrams of lower (Miramichi Group) and upper (Nepisiguit Falls Fm) sedimentary rocks from DDH HSB3409, as well as a bulk sample of the lower and upper sedimentary rock packages (large symbols).

the alteration zone relative to determined background values. In addition, Cu, Pb, Zn, Co, Ag, Cr, and P contents in the footwall increase with increasing intensity of chloritic alteration toward the massive sulfide deposit (Figs. 9a, b).

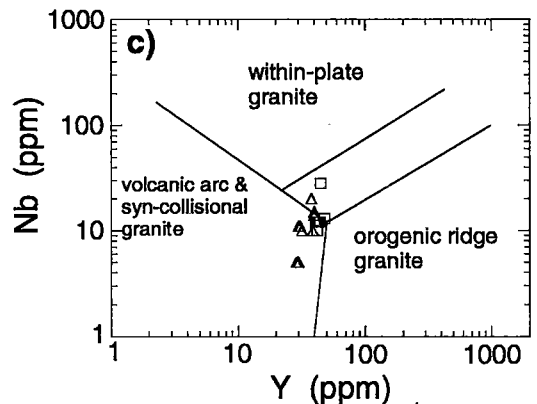
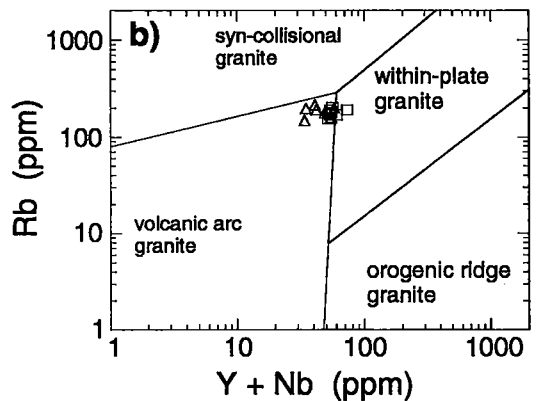
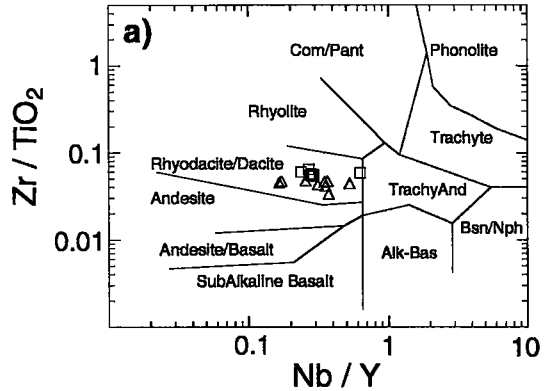


FIG. 12. Geochemical compositions of the FW and HW CT of the Nepisiguit Falls Formation. a) Zr/TiO_2 versus Nb/Y compositional discrimination diagram (Winchester & Floyd 1977), b) Rb versus $Y + Nb$, and c) Nb versus Y tectonic discrimination diagrams for granitic rocks (Pearce *et al.* 1984).

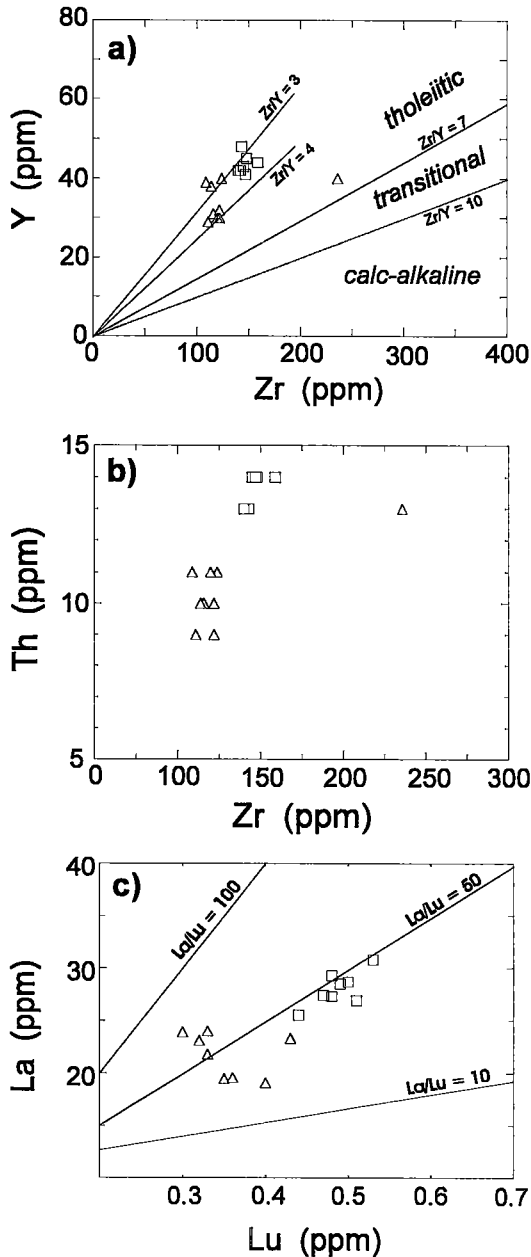


FIG. 13. Geochemical compositions of the FW and HW CT of the Nepisiguit Falls Formation. a) Y versus Zr variation diagram (Barrett & MacLean 1994), b) Th versus Zr, and c) La versus Lu variation diagrams. Symbols as in Figure 10.

Footwall (FW) alteration

The identity of the original feldspar phenocrysts is uncertain. In the footwall, microcline has been replaced by albite or phyllosilicates or both, but high in the hanging wall, coarse translucent albite is partially altered to microcline. The nature of these low-temperature feldspathization reactions is not well understood. In any case, the least-altered rocks have intermediate Na/K contents within the normal igneous spectrum of Hughes (1973) (Fig. 15).

The intensity of the chloritic alteration, and the iron contents of chlorite, increase toward the exhalative horizon. In the relatively homogeneous footwall CT, there is a transition from QFCT to QCT. In thin section, the microcline is partially replaced by albite, and less commonly by chlorite and sericite. The albite has poorly formed albite twins that are locally chessboard-textured, and is, in turn, replaced by quartz–chlorite–sericite that mimics the original alkali feldspar crystal in habit and size (see also Lentz & Goodfellow 1993a). The hydrolysis of albite marks the almost complete removal of sodium from the rock (Fig. 15). Analogous to the Brunswick No. 12 deposit, the QCT, or lower quartz porphyry in mine terminology, represents an alteration product of the QFCT and occurs along its upper contact adjacent to the upper footwall sedimentary package.

The upper footwall sedimentary rocks are very similar mineralogically to the altered footwall QCT, except they are generally devoid of phenocrysts and have a higher proportion of chlorite. These two rock types are chemically very similar, but on the basis of immobile elements and ratios of immobile elements (MacLean 1990, MacLean & Barrett 1993), the sedimentary rocks are compositionally more heterogeneous. The higher proportion of chlorite in the sedimentary rocks results in lower SiO₂, K₂O, and MnO, and higher MgO and Fe₂O₃ (total) contents (Fig. 9a). K₂O, Ba, Rb, and Sr contents decrease gradually toward the massive sulfides (Fig. 9a). The enrichment in total Fe coincides with increasing S contents from disseminated pyrite and, to a lesser extent, pyrrhotite, chalcopyrite and sphalerite. CO₂ and CaO contents are generally low. As with Al₂O₃, most other immobile elements (Ti, Zr, Th, HREE, Y, and Sc, Fig. 9a) are diluted. Overall, there is approximately 30 to 50% mass addition in the most-altered footwall samples if Al is considered immobile (*cf.* Lentz & Goodfellow 1993a). As mentioned earlier, the footwall sedimentary rock at the top of the package (samples 16 and 17) may be more aluminous (pelagic?), which would make the calculated mass-change values underestimates. Nonetheless, these mass-change values are high and typical of chloritites in footwall sedimentary rocks at Brunswick No. 12 (see data in Leitch & Lentz 1994), but are considerably less than the intensely silicified (up to 300% mass addition) footwall sedimentary rocks that occurs in the near-surface core of the discharge system (Lentz & Goodfellow 1996).

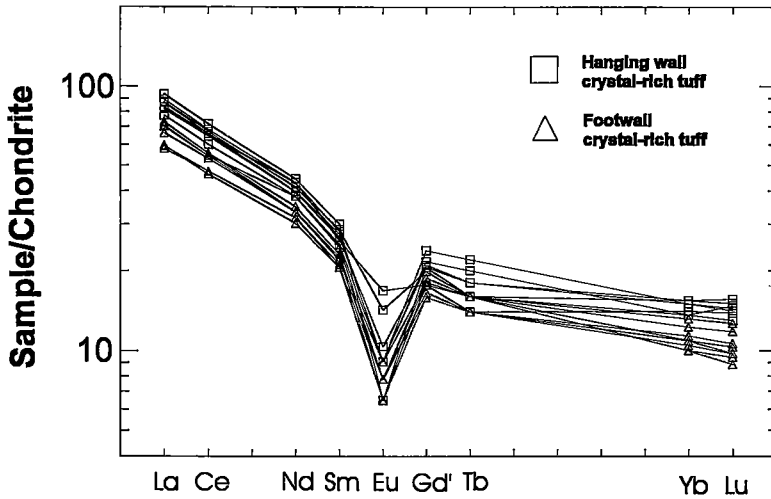


FIG. 14. Chondrite-normalized rare-earth-element (REE) abundances for the FW and HW CT. Values used in normalization are from Anders & Ebihara (1982). Gd was calculated by a Sm–Tb interpolation (Gd').

The Co, Cu, As, and Sb contents progressively increase toward the massive sulfide lens (Fig. 9b), which, at Brunswick No. 12, was interpreted (Lentz & Goodfellow 1993c) to reflect the high temperature-dependent solubility of

Cu/(Cu + Pb + Zn) value increases from 0.1 to near 1 within 50 m of the massive sulfide lens. Au is also slightly enriched (20 times background). The Eu/Eu* ratio increases continually toward the ore horizon. This pattern of enrichment has also been identified at the Halfmile Lake deposit to the west (Adair 1992, Lentz 1996b) and correlates strongly with Pb.

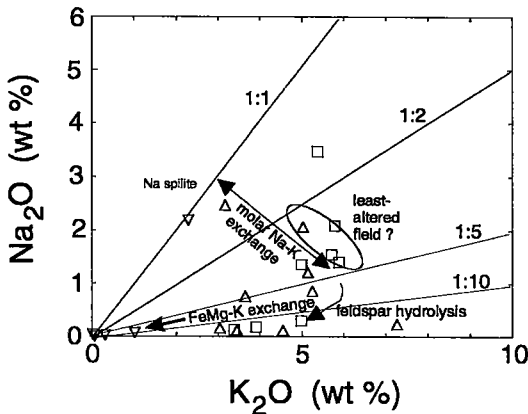


FIG. 15. K_2O versus Na_2O diagram illustrating the range in alkali compositions of the FW volcaniclastic and sedimentary rocks (NF Fm) and HW volcaniclastic rocks (NF Fm). A least-altered field is illustrated on the basis of petrographic observations. Vectors of Na–K exchange, and Fe + Mg – K exchange show the principal alteration processes that acted on these rocks. Symbols as in Figure 10.

their respective sulfide phases (Heinrich & Eadington 1986, Wood *et al.* 1987). Zn, Pb, Hg, and Sn contents also increase, but are locally erratic, like in the alteration zone at Brunswick No. 12 (Lentz & Goodfellow 1993c). The

In Figure 9b, the Fe/(Fe + Mg) value increases from 0.5 to 0.9 upward in the footwall CT, decreases sharply into the upper footwall sediment package, and then increases toward the massive sulfides. Similarly, K/(K + Na) increases from the least-altered CT to the QCT, decreases in sample 012, but otherwise remains elevated. The CIA [$Al_2O_3/(Al_2O_3 + Na_2O + K_2O)$, molar] increases progressively from 0.55 (least-altered) to 1 at the ore horizon, which indicates a leaching of alkali elements. Like the alteration index, (Fe + Mg)/(K + Na) increases progressively toward the ore horizon, from values <1 to almost 100, indicative of increasing chlorite at the expense of mica and feldspars. The Fe/Mn value consistently increases from near 10 to >200 near the ore horizon, similar to Whitehead's (1973) observations. The Mg/Ca value increases irregularly from about 3 in the least-altered rocks to nearly 20 in the altered rocks.

Overall, the footwall alteration described herein and by Wahl (1978) is less intense than that found at the A, C, and D zones. The less intense stringer-sulfide mineralization, the continuity of chloritic alteration in the footwall, and the general absence of silicic near-vent alteration, as at Brunswick No. 12, indicate that the deposit is extremely attenuated, as inferred by de Roo *et al.* (1991) and Moreton (1994). However, it is still considered a proximal-autochthonous deposit (Jambor 1979) on the basis of the intensity of chloritization and the Cu-rich base to much of the deposit.

Hanging-wall (HW) alteration

The hanging-wall unit is texturally homogeneous, although within 50 m of the sulfide contact, alteration has removed the alkali feldspar from the QFCT. There is a transition zone about 5 m wide characterized by the decreasing size of whitish alkali feldspar. In contrast to the footwall, quartz–mica pseudomorphs are absent;

chessboard albite is partially replaced by turbid alkali feldspar and *vice versa*.

The QCT and QFCT have identical immobile-element contents and ratios, such as Zr/TiO₂, Nb/Y, and La/Lu (Fig. 9b). As in the footwall, there is a considerable decrease in Na, K, Ca, Rb, and Sr (Fig. 9a) toward the ore horizon, consistent with chloritization. Fe–Mn–Mg–S covariations (Fig. 9a) indicate that the Fe in the altered

TABLE 1. COMPOSITIONAL AVERAGES OF VARIOUS ROCK UNITS IN DRILL HOLE HSB3409, HEATH STEELE B ZONE VMS DEPOSIT, NEW BRUNSWICK

Sample n	LFWs		FWCT		UFWs		HWCT		LFWs		UFWs	
	3		9		5		8		bulk*	bulk**		
wL%	\bar{x}	1s	\bar{x}	1s	\bar{x}	1s	\bar{x}	1s	\bar{x}	1s	\bar{x}	1s
SiO ₂	58.6	5.4	73.2	3.0	61.0	14.9	73.4	1.03	61.5	66.2	1.12	0.68
TiO ₂	1.04	0.08	0.31	0.15	0.55	0.11	0.25	0.02	1.12	0.88	1.12	0.68
Al ₂ O ₃	19.73	3.07	13.1	0.88	9.35	2.76	13.03	0.53	17.7	13.9	17.7	13.9
Fe ₂ O ₃	8.89	0.84	3.87	1.88	20.16	11.30	2.56	1.20	7.96	9.56	7.96	9.56
MnO	0.07	0.01	0.12	0.07	0.07	0.03	0.03	0.02	0.08	0.06	0.08	0.06
MgO	2.25	0.19	1.20	0.49	2.24	1.11	1.52	0.61	1.93	1.72	1.93	1.72
CaO	0.25	0.10	0.41	0.39	0.18	0.08	0.41	0.16	0.28	0.29	0.28	0.29
Na ₂ O	2.10	0.54	0.89	0.88	0.47	0.97	1.31	1.14	1.75	0.26	1.75	0.26
K ₂ O	3.58	0.71	4.51	1.35	0.75	0.95	5.00	0.92	3.33	3.32	3.33	3.32
P ₂ O ₅	0.10	0.04	0.13	0.01	0.09	0.04	0.13	0.01	0.08	0.14	0.01	0.08
H ₂ O ⁺	3.3	0.5	1.7	0.5	3.4	1.0	1.35	0.62	3.1	3.0	3.1	3.0
CO ₂	0.05	0.01	0.10	0.14	0.03	0.02	0.31	0.36	0.08	0.12	0.08	0.12
S	1.00	0.16	0.24	0.31	4.6	5.3	0.05	0.07	0.86	1.09	0.07	0.86
ppm												
Ag	0.25	0.00	0.31	0.18	1.4	0.5	0.45	0.42	0.4	<0.1	0.42	0.4
As	20	28	7	9	157	137	1.4	0.7	7.1	38.0	7.1	38.0
Au	1.8	1.9	2.3	4.4	18.7	18.8	0.8	0.5	<2	7	0.5	<2
B	40	7	8	5	5	0	8	5	19	13	5	19
Ba	496	75	659	367	134	179	1347	1070	466	364	466	364
Be	5.7	0.6	3.0	0.7	3.2	1.1	3.1	0.6	4	3	0.6	4
Bi	4.3	4.9	3.2	2.3	103	109	2.7	1.8	0.8	4.8	1.8	0.8
Br	1.7	0.6	2.0	0.5	2.0	0	1.6	0.5	4	3	0.5	4
Co	19	2	3.5	2.8	153	142	2	2	18	38	2	18
Cr	80	18	10	3.3	27	18	8	2	84	38	2	84
Cs	4.7	1.2	2.7	0.9	1.2	1.0	2.8	1.5	4	3	1.5	4
Cu	49	12	17	21	1343	1160	9	15	52	77	9	15
Hf	4.7	0.6	4.0	1.3	4.6	2.3	4.1	0.35	7.3	7.6	0.35	7.3
Hg	2.5	0.0	3.9	3.0	7.0	6.9	9.1	10.9	<5	7	10.9	<5
Li	17	2	7	3	5	0	6.8	3.3	7	4	3.3	7
Nb	17	0.6	11	5	12.6	9.0	13.9	5.8	20	16	5.8	20
Ni	44	8	6	2	14.6	9.2	3.6	0.9	39	13	0.9	39
Pb	2.0	1.7	34	59	13.4	16.6	371	711	2	2	711	2
Pd	0.7	0.3	2.6	1.9	1.4	1.1	0.5	0	-	-	0	-
Pt	5	0	11	5	7.4	3.4	5	0	-	-	0	-
Rb	160	33	182	22	37	43	179	15	159	155	15	159
Sb	0.7	0.2	0.52	0.39	4.4	5.0	3.5	6.0	0.6	1.9	6.0	0.6
Sc	19.4	4.3	5.1	4.6	9.4	3.5	4.1	0.2	16	10	0.2	16
Sn	8.7	6.4	13	5	93	158	12	5	13	27	5	13
Sr	97	22	56	21	21	17	61	22	93	29	22	93
Th	14.0	2.6	10.4	1.2	7.6	2.2	13.5	0.5	16.0	13.0	0.5	16.0
U	4.5	1.1	4.2	0.5	2.2	0.8	4.8	0.3	4.9	4.4	0.3	4.9
V	134	24	25	24	55	20	15	1	130	67	1	130
W	3.1	1.4	2.1	1.0	2.6	1.1	2	1	2	3	1	2
Y	37	2	34	5	27.8	12.0	43	2	43	37	2	43
Zn	122	14	504	807	96	60	592	987	149	738	987	149
Zr	180	23	130	40	192	86	146	6	257	213	6	257
La	48.7	53.9	23.8	6.5	35.2	10.2	28.1	1.6	50.5	35.9	1.6	50.5
Ce	94.3	12.7	48.6	11.9	68.8	19.6	57.1	2.9	105	76.0	2.9	105
Nd	42.0	5.2	22.7	5.2	31.4	10.1	26.1	1.4	46.7	33.1	1.4	46.7
Sm	8.1	1.3	4.8	1.0	6.4	2.0	5.6	0.3	9.2	7.3	0.3	9.2
Eu	1.73	0.31	0.68	0.31	3.12	1.91	0.83	0.26	1.49	2.05	0.26	1.49
Tb	1.1	0.1	0.8	0.1	0.7	0.2	0.89	0.13	1.4	1.1	0.13	1.4
Yb	3.4	0.3	2.6	0.5	2.5	0.9	3.2	0.17	4.0	3.5	0.17	4.0
Lu	0.50	0.06	0.37	0.07	0.37	0.15	0.49	0.03	0.59	0.49	0.03	0.59

Notes: LFWs: lower footwall sediments, UFWs: upper footwall sediments, FWCT: footwall crystal tuff, HWCT: hanging-wall crystal tuff. Fe_2O_3 is the expression of total iron. \bar{x} : mean, 1s: one standard deviation, n: number of samples analyzed. bulk*: 8 samples at 50 m intervals (10 cm long), bulk**: 6 samples at 50 m intervals (10 cm long). -: no analysis. The rocks were analyzed at X-Ray Assay Laboratories using a multi-element package. Concentrations of the major elements and Ba, Nb, Rb, Sr, Y, and Zr were determined by X-Ray Fluorescence Spectroscopy (XRF) on fused disks. The concentration of Sn was determined by pressed powder XRF, that of Au, by fire assay Direct Coupled Plasma, and that of Li, Be, B, V, Co, Ni, Cu, Zn, Ge, Mo, Ag, Cd, Pb, and Bi, by inductively coupled emission spectroscopy (ICP-ES). The concentration of Sc, Cr, Sb, Cs, REE, Hf, Ta, W, Th, and U was determined by instrumental neutron activation analysis (INAA). The proportion of FeO was determined by ammonium metavanadate titration, S, by the Leco method, CO_2 by the coulometry method, and H_2O^+ by the Penfield method. The accuracy of the analyses was determined from an internal standard (94-RHY, Lentz 1995a). The XRF-determined major elements are typically within 2% of the recommended value, and concentrations of the trace elements (XRF) are within 5% of the accepted values, except for CaO and Sr, which are present at low concentrations. The remaining trace elements are within 15% of the accepted values, except for Sn, Bi, Ag, Zn, and Ni, which are below their detection limit in the standard for the analytical method used.

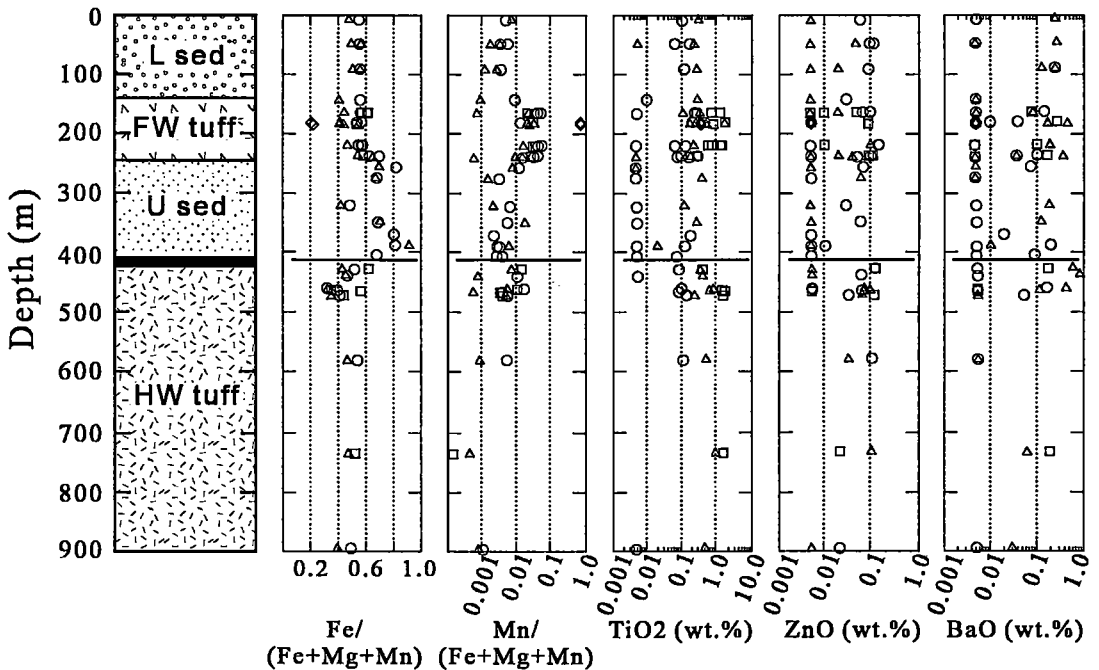


FIG. 16. Mineral compositional profiles along DDH HSB3409 illustrating Fe/(Fe + Mg + Mn), Mn/(Fe + Mg + Mn), TiO_2 , ZnO, and BaO contents of chlorite (○), phengite (△), biotite (□), and garnet (◇), as determined from results of electron-microprobe analyses (Table 2).

hanging-wall is mainly present as pyrite, with less in the chlorite [$\text{Fe}/(\text{Fe} + \text{Mg}) < 0.5$]. Barium contents in the altered CT are locally 2 to 5 times background, reflecting Ba-bearing phengitic muscovite (samples 18, 19, 20). Levels of Co, Cu, Zn, Pb, Sb, and Hg increase with sulfur toward the massive sulfides, but $\text{Cu}/(\text{Cu} + \text{Pb} + \text{Zn})$ decreases toward the ore zone (Fig. 9b). There is a slight increase in the Eu/Eu^* value

(0.4 to 1) toward the ore horizon (Fig. 9b). The ratio $\text{K}/(\text{K} + \text{Na})$ increases from the least-altered to most-altered rocks (Fig. 9b). The ratio $(\text{Fe} + \text{Mg})/(\text{K} + \text{Na})$ increases from least-altered (0.3) toward the ore horizon (Fig. 9b). The ratio Mg/Ca increases five-fold toward the ore zone (Fig. 9b). All the chemical changes observed are consistent with hydrolysis of feldspar and an increasing proportion of chlorite and pyrite to white mica toward the ore zone.

TABLE 2a. SELECTED RESULTS OF ELECTRON-MICROPROBE ANALYSES OF CHLORITE IN SAMPLES FROM DRILL HOLE HSB3409, HEATH STEELE B ZONE VMS DEPOSIT, NEW BRUNSWICK

No.	1	3	4	5	6	8	9	10	11	12	13	14	15	16	17	18	19	20	21	22	23	25
SiO ₂	24.40	24.24	24.78	24.13	27.50	25.51	25.63	24.12	22.80	23.98	24.75	23.08	22.10	22.82	24.31	24.58	25.44	27.76	26.92	27.36	25.62	26.74
TiO ₂	0.10	0.12	0.01	0.00	0.46	0.14	0.10	0.08	0.00	0.00	0.00	0.00	0.18	0.12	0.00	0.08	0.00	0.10	0.08	0.13	0.10	0.00
Al ₂ O ₃	22.66	23.42	21.82	21.49	17.86	19.27	19.92	20.30	21.87	21.27	21.80	22.94	23.21	22.46	20.49	21.51	21.01	20.52	19.96	19.23	19.83	19.87
FeO	28.16	28.40	29.18	29.16	28.80	29.98	31.73	32.04	39.60	34.81	25.76	33.83	38.18	38.49	34.29	27.17	24.69	18.36	22.07	22.35	28.63	26.76
MnO	0.25	0.19	0.48	2.58	0.75	2.28	2.13	1.69	0.57	0.16	0.35	0.26	0.10	0.14	0.13	0.00	0.52	0.84	0.20	0.27	0.24	0.05
ZnO	0.08	0.09	0.03	0.1	0.01	0.15	0.01	0.1	0.01	0.01	0.03	0.06	0.01	0.01	0.01	0.12	0.08	0.01	0.01	0.03	0.10	0.02
MgO	12.75	12.29	12.36	11.23	13.28	11.17	9.33	9.94	4.51	8.98	15.42	8.48	5.20	4.91	9.04	14.55	15.87	21.54	19.39	18.25	13.90	15.44
CaO	0.03	0.02	0.02	0.02	0.26	0.01	0.01	0.03	0.01	-	0.01	0.03	0.03	-	0.05	0.02	0.03	0.03	0.03	0.03	0.06	-
Na ₂ O	0.06	0.00	0.00	0.00	0.07	0.00	0.15	0.00	0.02	0.05	0.01	0.00	0.00	0.08	0.02	0.00	0.05	0.01	0.00	0.00	0.01	0.00
K ₂ O	0.00	0.01	0.00	0.00	0.26	0.00	0.15	0.00	0.00	0.00	-	0.00	0.00	0.00	0.00	0.00	0.00	0.00	0.00	0.00	0.07	0.00
H ₂ O	11.30	11.33	11.26	11.12	11.25	11.11	11.01	10.99	10.63	10.95	11.37	10.99	10.76	10.75	10.96	11.37	11.49	11.82	11.67	11.62	11.29	11.44
F	0.05	-	0.00	0.02	0.03	0.00	0.05	0.00	0.08	0.00	0.14	0.03	0.00	0.00	0.03	0.00	0.00	-	0.00	0.08	0.00	0.00
Cl	0.02	-	-	0.01	0.01	0.01	0.01	0.03	-	0.02	-	-	-	0.01	-	0.01	0.01	0.14	-	0.01	-	-
O=F	0.02	-	0.00	0.01	0.01	0.00	0.02	0.00	0.03	0.00	0.06	0.01	0.00	0.00	0.01	0.00	0.00	-	0.00	0.03	0.00	0.00
O=Cl	0.00	-	-	0.00	0.00	0.00	0.00	0.01	-	0.00	-	-	0.00	-	-	0.00	0.00	0.03	-	0.00	-	-
SUM	99.8	100.0	99.8	99.8	100.5	99.5	100.2	99.2	100.1	100.2	99.6	99.7	99.8	99.8	99.3	99.3	99.1	101.1	100.3	99.3	99.8	100.4
%Si	2.59	2.56	2.64	2.61	2.91	2.77	2.78	2.65	2.56	2.62	2.81	2.53	2.47	2.55	2.68	2.61	2.68	2.77	2.75	2.84	2.73	2.79
%Al	1.41	1.44	1.36	1.39	1.09	1.23	1.22	1.35	1.44	1.38	1.39	1.47	1.53	1.45	1.32	1.39	1.32	1.23	1.25	1.16	1.27	1.21
%Tsite	4	4	4	4	4	4	4	4	4	4	4	4	4	4	4	4	4	4	4	4	4	4
%Al	1.43	1.48	1.38	1.34	1.14	1.23	1.32	1.28	1.46	1.35	1.31	1.48	1.53	1.51	1.33	1.31	1.29	1.19	1.16	1.18	1.22	1.24
Ti	0.01	0.01	0.00	0.00	0.04	0.01	0.01	0.01	0.00	0.00	0.00	0.00	0.02	0.01	0.00	0.01	0.01	0.01	0.01	0.01	0.01	0.00
Fe ²⁺	2.50	2.51	2.60	2.63	2.55	2.72	2.88	2.95	3.72	3.18	2.27	3.10	3.57	3.60	3.16	2.41	2.18	1.53	1.89	1.94	2.55	2.33
Mn ²⁺	0.02	0.02	0.04	0.24	0.07	0.21	0.20	0.16	0.05	0.01	0.03	0.02	0.01	0.01	0.01	0.00	0.05	0.07	0.02	0.02	0.02	0.00
Mg	2.02	1.94	1.96	1.81	2.10	1.81	1.51	1.63	0.76	1.46	2.42	1.38	0.87	0.82	1.48	2.31	2.49	3.21	2.96	2.82	2.21	2.40
Ca	0.00	0.00	0.00	0.00	0.03	0.00	0.00	0.00	0.00	-	0.00	0.01	0.00	0.00	0.00	-	0.01	0.00	0.00	0.00	0.01	-
Na	0.01	0.00	0.00	0.00	0.01	0.00	0.03	0.00	0.00	0.01	0.00	0.00	0.00	0.02	0.00	0.00	0.01	0.00	0.00	0.00	0.00	0.00
K	0.00	0.00	0.00	0.00	0.04	0.00	0.02	0.00	0.00	0.00	-	0.00	0.00	0.00	0.00	0.00	0.00	0.00	0.00	0.00	0.01	0.00
Osite	5.99	5.97	5.99	6.03	5.96	5.99	5.97	6.03	5.99	6.02	6.04	6.00	5.99	5.97	6.00	6.04	6.02	6.01	6.04	5.98	6.02	5.98
O	10	10	10	10	10	10	10	10	10	10	10	10	10	10	10	10	10	10	10	10	10	10
OH	7.98	8.00	8.00	7.99	7.99	8.00	7.98	7.99	7.97	7.99	7.95	7.99	8.00	8.00	7.99	8.00	7.98	8.00	7.98	8.00	7.97	8.00
F	0.02	-	0.00	0.01	0.01	0.00	0.02	0.00	0.03	0.00	0.05	0.01	0.00	0.00	0.01	0.00	0.00	-	0.00	0.03	0.00	0.00
Cl	0.00	-	-	0.00	0.00	0.00	0.00	0.01	-	0.00	-	-	0.00	-	-	0.00	0.00	0.02	-	0.00	-	-

NOTES: The proportion of H₂O was calculated from the mineral formula. A JEOL-733 Superprobe with 15 kV accelerating voltage and 10 nA beam current was used with a maximum 40-second counting interval. Analytical results were corrected for matrix effects using the CITZAF program. The remainder of the data is deposited and is available from CISTL.

These features of alteration in the hanging wall occur on a much smaller scale than alteration at the ACD Zones (Wahl 1978) and the Brunswick No. 12 deposit (Lentz & Goodfellow 1994b). The 50-m-wide alteration halo may be considerably attenuated owing to strain within these "weakened" rocks. Hanging-wall alteration at the Heath Steele B Zone could be related to continued hydrothermal reaction after the CT was deposited (*cf.* the Millenbach deposit, Riverin & Hodgson 1980) or to diagenetic processes.

SYSTEMATIC VARIATIONS IN MINERAL COMPOSITIONS

Introduction

The foliated and recrystallized groundmass of all the rock types consists of variable proportions of quartz, K-rich white mica, biotite, stilpnomelane, and garnet, as well as feldspars in the less-altered samples. Many of the same minerals occur in the partially altered feldspar crystals and tensional pull-aparts and were analyzed for comparison. The chemical compositions of chlorite, white mica, biotite, and garnet were determined (Table 2). Locally, the very fine grain-size of some phases precluded chemical analysis.

Feldspar

Weakly turbid K-feldspar is locally preserved in the footwall CT. Tartan twinning, indicative of microcline, is locally evident and seems to replace the optically homogeneous alkali feldspar. At Brunswick No. 6, the optically homogeneous alkali feldspar is ordered microcline (Nelson 1983). In most of the footwall CT, alkali feldspar is partially to totally replaced by irregularly oriented, twinned albite crystals (An_{<3}; optical determination) and chlorite showing bluish interference colors. In the intensely altered rocks, albite and any remaining alkali feldspar are pseudomorphically replaced by a quartz-sericite-chlorite assemblage, which form milky quartz-rich augen. These milky quartz augen are different from the vitreous high-temperature quartz crystals analogous to the two varieties of quartz augen described at the Brunswick No. 12 deposit (Lentz & Goodfellow 1993a).

In the hanging-wall QFCT, the crystals of alkali feldspar are turbid, with patches of albite (chessboard textured, not turbid) locally preserved. Such textures are normally interpreted to result from albitization of K-feldspar (Battey 1955, Starkey 1959, Nelson 1983).

TABLE 2b. SELECTED RESULTS OF ELECTRON-MICROPROBE ANALYSES OF MUSCOVITE IN SAMPLES FROM DRILL HOLE B3409, HEATH STEELE B ZONE VMS DEPOSIT, NEW BRUNSWICK

No.	1	3	4	6	8	10	12	14	15	18	19	20	21	23	25
SiO ₂	47.64	45.73	47.80	47.80	50.60	47.60	47.28	46.00	45.28	49.28	47.59	47.98	49.26	48.14	49.43
TiO ₂	0.30	0.27	0.29	0.25	0.24	0.00	0.41	0.27	0.02	0.33	0.39	0.81	0.61	0.48	0.50
Al ₂ O ₃	34.90	34.27	31.89	29.88	29.00	28.33	30.74	35.24	35.37	30.31	29.78	26.91	27.43	30.13	28.82
Fe ₂ O ₃	-	0.00	0.00	0.00	0.00	-	0.00	-	0.00	0.00	0.00	-	0.00	0.00	-
FeO	2.07	1.96	2.17	3.59	3.31	5.18	4.38	2.43	3.23	3.06	3.23	4.01	3.39	3.21	2.73
MnO	0.03	0.00	0.00	0.18	0.12	0.09	0.01	0.06	0.02	0.05	0.00	0.06	0.00	0.00	0.00
MgO	1.25	1.03	1.73	2.73	2.01	2.09	1.22	0.54	0.16	2.27	2.19	4.61	3.66	2.10	2.33
BaO	0.26	0.27	0.00	0.00	0.21	0.39	0.00	0.13	0.01	0.62	0.87	0.41	0.11	0.00	0.03
CaO	0.02	0.01	-	0.06	0.06	-	0.01	0.02	0.01	0.01	-	0.04	0.01	-	0.04
Na ₂ O	0.38	0.47	0.20	0.27	0.20	0.00	0.27	0.54	0.74	0.33	0.27	0.16	0.12	0.18	0.17
K ₂ O	9.68	9.27	10.49	9.27	10.13	10.94	10.61	9.89	9.71	10.10	10.43	10.76	10.72	10.94	11.05
H ₂ O	4.52	4.38	4.50	4.45	4.49	4.40	4.41	4.50	4.46	4.29	4.29	4.44	4.46	4.45	4.47
F	0.00	0.28	0.00	0.00	0.00	0.00	0.00	0.00	0.05	0.38	0.30	0.00	0.00	0.04	0.00
Cl	-	0.01	-	0.15	0.01	-	0.11	-	-	-	0.01	-	-	-	0.01
O=F	0.00	0.12	0.00	0.00	0.00	0.00	0.00	0.00	0.02	0.16	0.13	0.00	0.00	0.02	0.00
O=Cl	-	0.00	-	0.03	0.00	-	0.02	-	-	-	0.00	-	-	-	0.00
SUM	101.1	97.8	99.1	98.6	100.4	99.0	99.5	99.6	99.0	100.9	99.2	100.2	99.8	99.7	99.6
^{IV} Si	6.25	6.21	6.42	6.48	6.73	6.55	6.42	6.15	6.11	6.55	6.48	6.51	6.64	6.49	6.65
^{VI} Al	1.75	1.79	1.58	1.52	1.27	1.45	1.58	1.85	1.89	1.45	1.52	1.49	1.36	1.51	1.35
Tsite	8	8	8	8	8	8	8	8	8	8	8	8	8	8	8
^{VI} Al	3.64	3.69	3.48	3.26	3.27	3.14	3.34	3.71	3.74	3.29	3.25	2.81	3.00	3.27	3.22
^{VI} Ti	0.03	0.03	0.03	0.03	0.02	0.00	0.04	0.03	0.00	0.03	0.04	0.08	0.06	0.05	0.05
Fe ³⁺	-	0.00	0.00	0.00	0.00	-	0.00	-	0.00	0.00	0.00	-	0.00	0.00	-
Fe ²⁺	0.23	0.22	0.24	0.41	0.37	0.60	0.50	0.27	0.36	0.34	0.37	0.45	0.38	0.36	0.31
Mn ²⁺	0.00	0.00	0.00	0.02	0.01	0.01	0.00	0.00	0.01	0.00	0.01	0.00	0.01	0.00	0.00
Mg	0.24	0.21	0.35	0.55	0.40	0.43	0.25	0.11	0.03	0.45	0.44	0.93	0.74	0.42	0.47
Osite	4.15	4.15	4.10	4.26	4.07	4.17	4.12	4.12	4.14	4.12	4.11	4.28	4.18	4.11	4.04
Ba	0.01	0.01	0.00	0.00	0.01	0.02	0.00	0.01	0.00	0.03	0.05	0.02	0.01	0.00	0.00
Ca	0.00	0.00	-	0.01	0.01	-	0.00	0.00	0.00	0.00	-	0.01	0.00	-	0.01
Na	0.10	0.12	0.05	0.07	0.05	0.00	0.07	0.14	0.19	0.08	0.07	0.04	0.03	0.05	0.04
K	1.62	1.60	1.80	1.60	1.72	1.92	1.84	1.69	1.67	1.71	1.81	1.86	1.84	1.88	1.90
Asite	1.73	1.74	1.85	1.68	1.79	1.94	1.91	1.84	1.87	1.83	1.93	1.88	1.88	1.93	1.95
O	20	20	20	20	20	20	20	20	20	20	20	20	20	20	20
OH	4.00	3.88	4.00	3.96	4.00	4.00	3.97	4.00	3.98	3.84	3.87	4.00	4.00	3.98	4.00
F	0.00	0.12	0.00	0.00	0.00	0.00	0.00	0.00	0.02	0.16	0.13	0.00	0.00	0.02	0.00
Cl	-	0.00	-	0.03	0.00	-	0.03	-	-	-	0.00	-	-	-	0.00

Notes: The proportion of H₂O was calculated from the mineral formula. See Table 2a for analytical method. The remainder of the data is deposited and is available from CISTI.

Farther into the hanging wall, Carlsbad-twinning chessboard albite (discontinuous albite twinning) is common, with networks of turbid alkali feldspar replacing plagioclase phenocrysts. The hydrothermal replacement of sodic plagioclase by turbid alkali feldspar can occur at low temperatures in the presence of a fluid having a high Na⁺/K⁺ (30), similar to modern seawater (Munhá *et al.* 1980); thus plagioclase was probably the liquidus feldspar. This conclusion contrasts with most other cases inferred for the Nepisiguit Falls Formation, but plagioclase phenocrysts have been described from the Clearwater Stream Formation to the southwest (Fyffe 1995); therefore, sodic rhyodacite (low-K) may have been present.

Chlorite

The color of the rocks in drill core reflects the proportion and iron content of chlorite. The most Fe-rich chlorite-enriched sedimentary rocks (very dark green in hand specimen) occur in the immediate footwall to the massive sulfides. The interference color of the chlorite

ranges from berlin blue to gold-brown, and is related to Fe:Mg value (Kranidiotis & MacLean 1987). The compositions (Figs. 16, 17) range from ferroan clinocllore to chamosite, using the nomenclature of Bayliss (1975) (see also Sutherland 1967, Lewczuk 1990, Luff *et al.* 1992, Lentz & Goodfellow 1993a).

At constant metamorphic grade, the phyllosilicate assemblage reflects the variation in bulk composition, although high sulfide content increases the Fe/(Fe + Mg) value of the whole rock relative to the ratio in minerals (Fig. 18).

The variation of ^{IV}Si in chlorite is a function of coupled Tschermak substitution ($M^{2+} + Si^{4+} = VIAl^{3+} + IVAl^{3+}$). The Al content of chlorite is also strongly affected by the availability of Al and degree of silica saturation of the rock. Therefore, covariation of Fe and Al probably reflects the variation in silica content (^{IV}Si < 2.6 atoms per formula unit, Fig. 17), proximity to pyrophyllite (kyanite) saturation in the most-altered rocks, and the crystal-chemical effects mentioned above. Lentz & Goodfellow (1993a) also noted that the

TABLE 2c. SELECTED RESULTS OF ELECTRON-MICROPROBE ANALYSES OF BIOTITE IN SAMPLES FROM DRILL HOLE B3409, HEATH STEELE B ZONE VMS DEPOSIT, NEW BRUNSWICK

No.	5	6	7	8	9	10	20	21	22	24
SiO ₂	35.4	35.6	34.2	35.5	39.1	35.8	38.2	35.4	37.3	37.5
TiO ₂	0.78	1.86	1.73	0.62	0.19	0.39	1.39	1.71	1.53	1.62
Al ₂ O ₃	18.81	16.62	17.79	17.94	17.62	18.22	16.40	16.83	16.19	16.09
Cr ₂ O ₃	-	-	-	-	0.06	-	-	-	-	-
FeO	21.82	21.11	23.94	21.19	22.20	25.07	14.41	21.80	17.45	20.73
MnO	1.30	1.21	1.01	1.44	1.06	0.52	0.40	0.12	0.14	0.00
MgO	8.23	9.47	10.28	9.05	8.10	8.44	15.19	9.77	12.69	10.92
ZnO	0.005	0.05	0.005	0.005	0.01	0.005	0.005	0.11	0.09	0.12
BaO	0.005	0.005	0.00	0.00	0.00	0.17	0.00	0.00	0.00	0.18
CaO	0.03	0.01	0.06	0.02	0.07	0.04	0.02	-	0.01	0.03
Na ₂ O	0.12	0.00	0.09	0.19	0.17	0.06	0.08	0.06	0.03	0.07
K ₂ O	9.27	8.63	6.28	9.25	6.81	8.20	9.94	9.36	9.78	9.65
H ₂ O	3.71	3.67	3.71	3.67	3.76	3.69	4.05	3.79	3.73	3.56
F	0.41	0.50	0.41	0.46	0.48	0.39	0.00	0.24	0.55	0.79
Cl	-	0.02	0.02	0.03	0.02	0.02	0.01	0.01	-	0.01
O=F	0.17	0.21	0.17	0.19	0.20	0.16	0.00	0.10	0.23	0.33
O=Cl	-	0.00	0.00	0.01	0.00	0.00	0.00	0.00	-	0.00
SUM	99.7	98.5	99.3	99.2	99.5	100.8	100.1	99.0	99.2	100.9
^{IV} Si	5.45	5.53	5.27	5.49	5.90	5.48	5.64	5.49	5.64	5.66
^{IV} Al	2.55	2.47	2.73	2.51	2.10	2.52	2.36	2.51	2.36	2.34
Tsite	8	8	8	8	8	8	8	8	8	8
^{VI} Al	0.86	0.57	0.50	0.76	1.03	0.76	0.50	0.56	0.53	0.52
Ti	0.09	0.22	0.20	0.07	0.02	0.04	0.15	0.20	0.17	0.18
Fe ³⁺	0.00	-	-	0.00	-	-	-	-	0.00	0.00
Fe ²⁺	2.81	2.74	3.08	2.74	2.80	3.21	1.78	2.82	2.21	2.61
Mn ²⁺	0.17	0.16	0.13	0.19	0.14	0.07	0.05	0.02	0.02	0.00
Mg	1.89	2.19	2.36	2.09	1.82	1.93	3.34	2.25	2.86	2.45
Osite	5.82	5.88	6.28	5.85	5.82	6.01	5.82	5.85	5.79	5.77
Ba	0.00	0.00	0.00	0.00	0.00	0.01	0.00	0.00	0.00	0.01
Ca	0.00	0.00	0.01	0.00	0.01	0.01	0.00	-	0.00	0.00
Na	0.04	0.00	0.03	0.06	0.05	0.02	0.02	0.02	0.01	0.02
K	1.82	1.71	1.23	1.83	1.31	1.60	1.87	1.85	1.89	1.86
Asite	1.86	1.71	1.27	1.89	1.37	1.64	1.90	1.87	1.90	1.89
O	20	20	20	20	20	20	20	20	20	20
OH	3.80	3.75	3.80	3.77	3.77	3.81	4.00	3.88	3.74	3.62
F	0.20	0.25	0.20	0.23	0.23	0.19	0.00	0.12	0.26	0.38
Cl	-	0.01	0.01	0.01	0.01	0.01	0.00	0.00	-	0.00

Notes: The proportion of H₂O was calculated from the mineral formula. See Table 2a for analytical method. The remainder of the data is deposited and is available from CISTI (see text for details). As in Tables 2a and 2b, results of the analyses are quoted in wt.%.

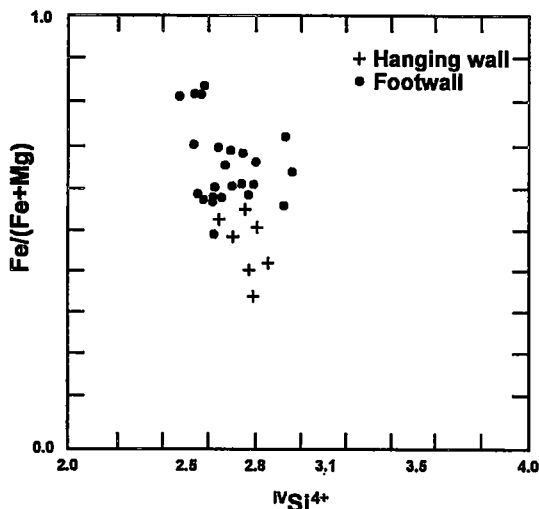


FIG. 17. $IVSi^{4+}$ versus $Fe/(Fe + Mg)$ in chlorite, illustrating the chlorite compositions in the HW and FW units (Table 2a).

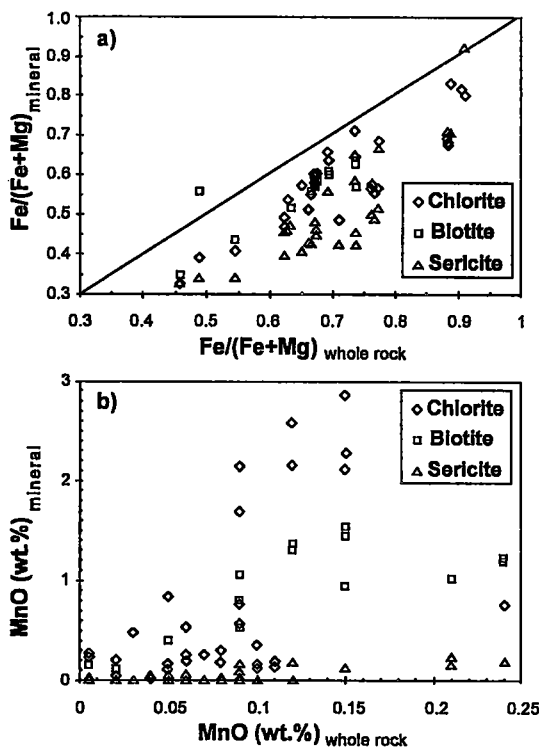


FIG. 18. Whole-rock versus mineral a) $Fe/(Fe + Mg)$ weight ratio and b) MnO contents.

proportion of $IVSi$ decreases and that of total Al increases with increasing alteration at Brunswick No. 12. Crystal-chemical effects related to Fe and Mg contents control the $IVAl$ content of chlorite (Kranidiotis & MacLean 1987). However, experimental data (Saccoccia & Seyfried 1994) show that the $IVAl$ content of chlorite is insensitive to temperature of formation.

Chlorite in the hanging wall has a lower $Fe/(Fe + Mg)$ value than that in the footwall. In both areas, chlorite becomes richer in Fe toward the ore horizon, although the trend is more pronounced in the footwall (Figs. 16, 17, Table 2). The background $Fe/(Fe + Mg + Mn)$ in chlorite increases near the exhalite, but decreases at the exhalite contact, where disseminated sulfides are abundant. The relatively low $Fe/(Fe + Mg)$ value of chlorite near the exhalite horizon (samples 16 and 17) is probably due to the higher $f(H_2S)$ (Bryndzia & Scott 1987), resulting in sulfide formation at the expense of ferrous iron in chlorite (see below).

The $Mn/(Fe + Mg + Mn)$ value of chlorite (Fig. 16) is low in the lower quartzose sedimentary package, but increases ten-fold in the CT unit of the footwall, and decreases to <0.01 in the upper footwall. In general, the Mn contents of chlorite, sericite and biotite reflect whole-rock Mn contents. The spessartine garnet (sample 006) in the footwall CT with the highest Mn content formed at the expense of Mn in some of the chlorite and possibly carbonates. The low-T enrichment of Mn in the least-altered rocks is consistent with the decreasing solubility of Mn relative to Fe with increasing temperature, based on fluid/chlorite distribution coefficients (Sverjensky 1985).

In the footwall, Zn contents of chlorite are also irregular (40 to 1200 ppm), although the highest values occur in some of the least-altered rocks (Fig. 16). This pattern may reflect the removal of Zn by leaching of altered rocks and its partition into sulfides at high sulfur fugacities. This is consistent with thermodynamic calculations for coexisting fluid and chlorite (Sverjensky 1985), which suggests that Zn partitions into a solution relative to Fe and Mg. At the Mount Lyell deposit, Hendry (1981) found that the Zn content of chlorite is also variable, but with a greater range, up to 5000 ppm. Mottl (1983) found 187 to 262 ppm Zn in chlorite from the mid-ocean ridges.

White mica

The white mica ranges from a muscovitic to a phengitic composition (Fig. 19, Table 2b). The most phengitic compositions are the most Mg-rich, indicative of the coupled Tschermak substitution ($M^{2+} + Si^{4+} = VIAl^{3+} + IVAl^{3+}$, Fig. 20), which favors the incorporation of Mg over Fe (Lentz & Goodfellow 1993a). With increasing alteration, there is an increase in Al toward end-member muscovite compositions (samples 011 to 015), as also documented at Brunswick No. 12 (Lentz & Goodfellow 1993a) and several other massive sulfide deposits (Hendry 1981, Urabe *et al.* 1983, Schmidt 1988). In general, the

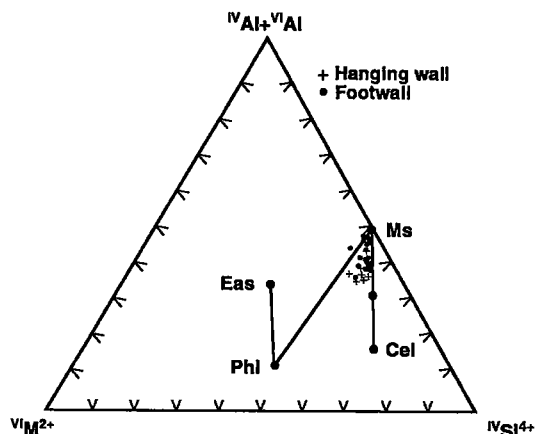


FIG. 19. ${}^{IV}Al + {}^{VI}Al - {}^{IV}Si$ triangular diagram (Monier & Robert 1986) illustrating the composition of white micas from the FW and HW (Table 2b). Eas: eastonite, Phl: phlogopite, Ms: muscovite, Cel: celadonite.

$Fe/(Fe + Mg + Mn)$ values of phengitic mica mimic the whole-rock compositions (Fig. 16). The $Mn/(Fe + Mg + Mn)$ value of muscovite is much less regular. TiO_2 contents typically range from 0.1 to 1 wt.% (Fig. 16). The highest Ti values coincide with the highest Si contents, which implies a relationship similar to phengite substitutions (${}^{VI}M^{2+} + {}^{VI}Ti^{4+} = 2 {}^{VI}Al^{3+}$; Guidotti 1984). In the footwall, Ba contents are very

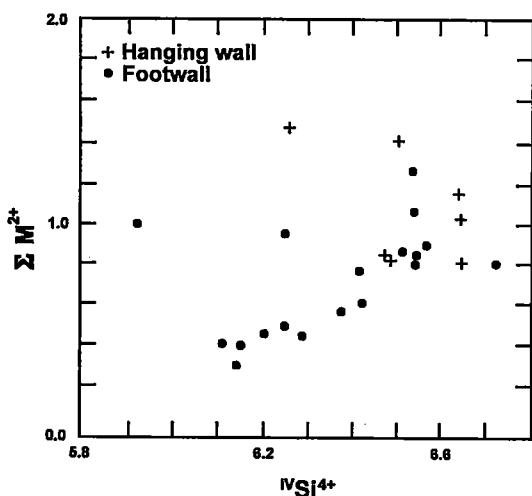


FIG. 20. Plot of ΣM^{2+} versus ${}^{IV}Si^{4+}$ of white micas illustrating general enrichment of divalent cations (Fe, Mg, Mn) with ${}^{IV}Si^{4+}$ contents that are related to Tschermak substitution.

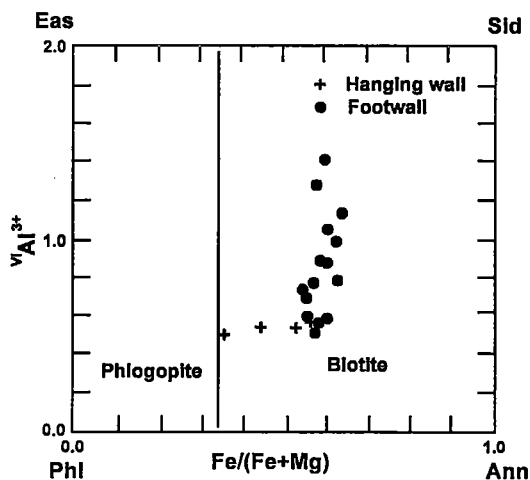


FIG. 21. Plot of $Fe/(Fe + Mg)$ versus ${}^{VI}Al^{3+}$ illustrating the composition of biotite from the FW and HW (Table 2c). Ann: annite, Phl: phlogopite, Sid: siderophyllite, Eas: eastonite.

irregular; values up to 0.5 wt.% BaO are common, but Ba contents decrease toward the ore horizon. The highest Ba contents of phengitic mica occur in the altered QCT of the hanging wall (0.7 to 0.9 wt.%), but the level of Ba decreases to values less than 0.1 wt.% BaO further into the hanging wall (Fig. 16).

The ${}^{IV}Si$ content of phengite coexisting with K-feldspar, quartz, and phlogopite [$X(Mg) = 0.6$] ranges between 3.25 and 3.32 atoms per formula unit, which corresponds to pressures of about 500 to 700 MPa (5 to 7 kbar), based on the phengite geobarometer (Massonne & Schreyer 1987). Sphalerite from the Heath Steele deposits contains 13.7 to 14.1 mole % FeS (Sutherland & Halls 1969), coexists with a pyrrhotite-pyrite assemblage, and indicates comparable pressures of approximately 600 MPa at an inferred temperature of 450°C, using the Toulmin *et al.* (1991) calibration.

Biotite

Biotite is locally present as a late to post- S_2 metamorphic phase. The $Fe/(Fe + Mg)$ value of biotite ranges between 0.35 and 0.65, with a considerable siderophyllite component in the Fe-rich member (Fig. 21, Table 2c). The Fe-Mg-Al contents reflect the whole-rock composition and the assemblage in which it formed. Similarly, $Mn/(Fe + Mg + Mn)$ values are generally comparable to those in chlorite. The Ti contents of biotite range between 0.5 and 2 wt.% TiO_2 , and are highest in biotite with the lowest $Fe/(Fe + Mg + Mn)$ value or highest Si content (Fig. 16). The extent of Ti incorporation is a function of composition, but also of metamorphic grade and whether a phase such as titanite or rutile is present (Guidotti 1984,

Lentz 1994). The inverse relationship between Ti and siderophyllite component implies that the Ti-Tschermak substitution ($M^{2+} + {}^{\text{VI}}\text{Ti}^{4+} = 2 {}^{\text{VI}}\text{Al}^{3+}$) controlled the Ti contents of the biotite. The Zn content of biotite varies greatly (40 to 1000 ppm), and is highest in the least-altered rocks, which suggests that its abundance is affected by leaching and sulfur fugacity.

Garnet

Although rare, garnet forms small euhedral porphyroblasts that overgrow the S_1S_2 fabric. It occurs in rocks with a relatively high Mn content, particularly within the footwall QFCT. The garnet is spessartine-rich, with less than 15% almandine component (Fig. 16). Spessartine-rich garnet in a quartz – albite – muscovite – biotite assemblage generally forms at temperatures greater than 400°C depending on bulk composition (cf. Symmes & Ferry 1992). The $X(\text{Mn})_{\text{rock}}$ is 0.08 for sample 006 [$X(\text{Mn}) = \text{Mn}/(\text{Fe} + \text{Mg} + \text{Mn})$]. At 500 MPa (5 kbar), such compositions can form garnet at temperatures slightly less than 400°C. The 21 mol.% almandine component in spessartine and the Fe/(Fe + Mn) value of coexisting chlorite (0.98), which is high, are consistent with a temperature of 490°C (Kretz 1993), although 450°C is more reasonable considering the absence of amphibole and the low Ca content of plagioclase.

INTER-MINERAL EQUILIBRIA

Introduction

The compositions described above were generally determined on assemblages of coexisting minerals. Although the minerals were usually in proximity, *i.e.*, within 1 mm, they were rarely in mutual contact. However, most minerals have compositions indicative of equilibrium on the scale of a thin section.

Element distributions are used to describe these systems in more detail. For major elements, element ratios, *e.g.*, Fe/(Fe + Mg), are used to compensate for the constant-sum effect, whereas this is not required for trace elements. However, if solid-solution effects change the makeup of the exchange site in the mineral, then the trace element should be normalized to the exchanging cation to define coherent distributions (*e.g.*, Rb/K). The actual distribution is described by the distribution coefficient, K_D (Kretz 1961). For major elements, the K_D is (eq. 1)

$$[\text{Fe}] K_D^{\text{Bt/Ms}} = [X_{\text{Fe}}^{\text{Bt}}(1 - X_{\text{Fe}}^{\text{Ms}})] / [(1 - X_{\text{Fe}}^{\text{Bt}})X_{\text{Fe}}^{\text{Ms}}] \quad [1]$$

where $[\text{Fe}] = \text{Fe}/(\text{Fe} + \text{Mg})$ for K_D , and $X_{\text{Fe}} = \text{Fe}/(\text{Fe} + \text{Mg})$.

The exchange of trace elements with various cations is best expressed as a simple ratio (eq. 2).

$$[\text{Zn}] K_D^{\text{Bt/Ms}} = \text{Zn}^{\text{Bt}}/\text{Zn}^{\text{Ms}} \quad [2]$$

The distribution of major-, minor-, and trace-element components describes the system in detail and assesses

the extent of equilibrium (or departures from it) between phases, and thus better defines the controls on alteration.

Chlorite – muscovite

The $[\text{Fe}] K_D^{\text{Chl/Ms}}$ values generally vary between 1.5 and 1 (Fig. 22a). These values are lower than those observed at Brunswick No. 12 ($[\text{Fe}] K_D^{\text{Chl/Ms}} = 1.68$; Lentz & Goodfellow 1993a) and Kidd Creek ($[\text{Fe}] K_D^{\text{Chl/Ms}}$ in the interval 2.0 to 2.5; Cameron *et al.* 1993), but similar to those around the Mount Lyell stockwork Cu deposit in

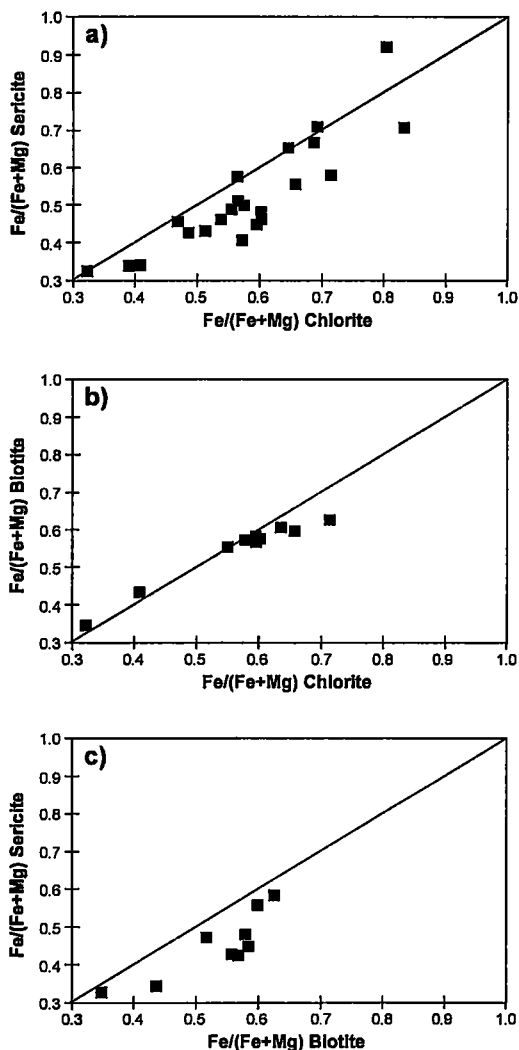


FIG. 22. Fe/(Fe + Mg) distribution $[\text{Fe}]$ between coexisting a) white mica and chlorite, b) biotite and chlorite, and c) white mica and biotite.

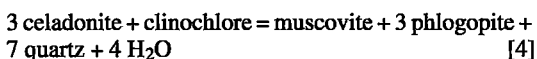
TABLE 3. $\delta^{18}\text{O}$ ISOTOPIC COMPOSITIONS (‰)
CRYSTAL TUFF, HEATH STEELE B ZONE

Sample	WR	GM	Qtz
4A	-	9.2	-
5A	-	7.5	10.2
6A	-	8.5	-
7	9.0	-	-
8	9.2	-	-
9	-	7.7	9.2
10	-	9.9	9.4
11	6.9	-	9.1
12	7.3	-	-
13	7.6	-	-
14	7.9	-	-
15	7.8	-	-
16	6.8	-	-
17	5.3	-	-
18	-	9.2	9.7
19	8.4	-	-
20	-	8.7	10.3
21	-	9.1	10.4
22	-	9.5	-
23	-	10.3	12.1
24	-	11.3	-
25	-	11.3	-

Notes: WR: whole-rock, GM: groundmass, Qtz: quartz phenocrysts. Using a binocular microscope, large (clear) phenocrysts of quartz and groundmass were separated by hand after fine crushing. The quartz phenocrysts were more than 80% pure. The oxygen isotopic compositions were determined at the Université de Montréal. Oxygen was liberated by reaction with BrF_3 (Clayton & Mayeda 1963). All $\delta^{18}\text{O}$ per mil (‰) values are reported relative to standard mean ocean water (SMOW: Craig 1961). NBS-28 quartz was used as an internal standard. In general, the analytical precision is within 0.2‰.

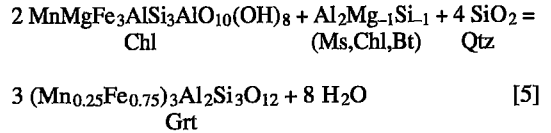
Biotite was not analyzed in several samples because of its fine grain-size; it is absent in the intensely chloritized rocks and the least-altered rocks. The presence of coexisting chlorite and muscovite suggests that the Fe-rich chlorite and end-member muscovite are stable under these conditions and that the biotite-forming reaction from these phases is incongruent.

The biotite – chlorite – muscovite geothermometer–geobarometer of Powell & Evans (1983) has been revised by Bucher-Nurminen (1987). This geothermobarometer is represented by contours of equilibrium coefficient ($\ln K$) of reaction 4:



In sample 20, the mole fractions of muscovite (0.65), phlogopite (0.60), celadonite (0.35), and clinochlore (0.68) with unit activity for K-feldspar and quartz at 450°C ($\ln K = 3.7$) correspond to a pressure of metamorphism between 350 to 400 MPa (3.5 and 4 kbar) for the assemblage at Heath Steele.

Crystallization of low-T metamorphic garnet is mainly a function of the Mn content in aluminous rocks. The probable garnet-forming reaction involves chlorite, quartz, and aluminous components of various other phases (eq. 5; Laird 1988):



This garnet-forming dehydration reaction is intended to represent the 21 mol.% almandine component in spessartine and corresponds to a temperature of formation of about 450°C.

OXYGEN ISOTOPE SYSTEMATICS

The $\delta^{18}\text{O}$ values of quartz separates from the footwall CT range from 9.1 to 10.2‰, whereas quartz from the hanging-wall CT range from 9.7 to 12.1‰ (Table 3, Fig. 25). The latter values approach the heavy $\delta^{18}\text{O}$ values (12.1‰) of the footwall CT from the Brunswick No. 12 deposit (Lentz & Goodfellow 1993a). Quartz separates from the altered rocks of both CT packages are isotopically lighter than in the least-altered samples, and may indicate isotopic modification of the quartz during hydrothermal alteration or partial re-equilibration during metamorphism. The difference in the isotopic composition of the quartz phenocrysts from the hanging-wall and footwall CT packages is consistent with our interpretation of these as separate lithological units. These differences are consistent with slightly different crustal sources for their respective melts, and involvement of isotopically heavy sedimentary rocks (O'Neil *et al.* 1977, Taylor 1980, Huston *et al.* 1996).

The whole-rock and groundmass $\delta^{18}\text{O}$ values of the footwall CT range from 7.5 to 9.9‰. The least-altered sample has a whole-rock composition of 9.2‰ (Table 3, Fig. 25). In the upper-footwall sedimentary package, whole-rock $\delta^{18}\text{O}$ values increase from 6.9 to 7.9‰ toward the ore horizon, coincident with weak silicification of the chloritic sediments, but decreases to 5.3‰ in the intensely chloritized sedimentary rocks directly beneath the deposit. In the hanging wall, the whole-rock and groundmass $\delta^{18}\text{O}$ values (8.4 to 11.3‰) increase with distance from mineralization, similar to the trend observed in the quartz separates (Table 3, Fig. 25).

In the least-altered CT from both footwall and hanging-wall sequences, the whole-rock and groundmass $\delta^{18}\text{O}$ values are consistently 1 to 2‰ lighter than the coexisting quartz separates, which is compatible with

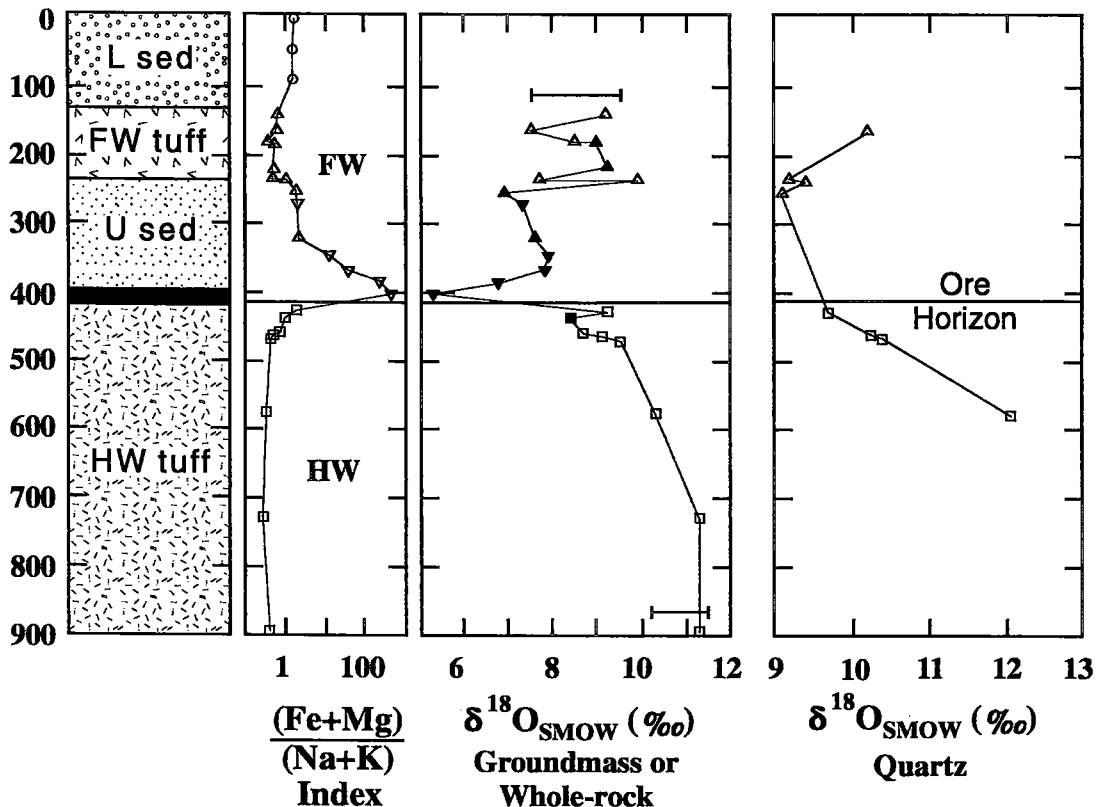


FIG. 25. Oxygen isotopic compositions ($\delta^{18}\text{O}$) of groundmass (open symbols) and whole rock (filled symbols), and quartz separates expressed relative to Vienna standard mean ocean water (VSMOW). The isotopic values are compared to the $(\text{Fe} + \text{Mg})/(\text{Na} + \text{K})$ alteration index and illustrated as profiles (Table 3). Symbols: lower sedimentary package (\circ), FW CT (\triangle), upper sedimentary package (∇), and HW CT (\square).

observations from other volcanic rocks (Taylor 1968, 1980). The isotopic data for the whole-rock and groundmass are consistent with the isotopic differences between the footwall and hanging wall defined by the quartz separates.

Whole-rock and groundmass $\delta^{18}\text{O}$ variations are principally related to mineralogical changes resulting from hydrothermal alteration and to variation in the isotopic composition and temperature of the fluid involved. In the least-altered tuffs, whole-rock SiO_2 contents decrease slightly with decreasing ^{18}O content (Fig. 26a), except for the extremely chloritized samples. The $\delta^{18}\text{O}$ decreases with K_2O , reflecting increasing degree of chloritic alteration (Fig. 26b). This also is reflected by a decrease in ^{18}O with increase in $\text{Al}_2\text{O}_3/(\text{Al}_2\text{O}_3 + \text{Na}_2\text{O} + \text{K}_2\text{O})$ (Fig. 26c) and increasing Fe_2O_3 (total) (Fig. 26d), partly due to increasing chlorite. These host-rock oxygen isotopic variations are similar to those from other altered samples in VMS deposits hosted by felsic volcanic rocks (e.g., Green *et al.* 1983, Barrett & MacLean 1991, MacLean & Hoy 1991, Hoy 1993, Huston *et al.* 1995).

Assuming a fractionation value $\Delta_{\text{chlorite-H}_2\text{O}}$ between chlorite and water of about 0 to -2‰ at an estimated formation temperature of 300 to 400°C, respectively (Wenner & Taylor 1971), the $\delta^{18}\text{O}$ value of the hydrothermal fluid in equilibrium with chlorite in sample 17 should be 5 to 7‰, i.e. well above the value for normal seawater. This high value is close to that inferred for the rock-dominated, ore-forming fluid at Brunswick No. 12 (4.0‰). Nonetheless, these positive values are consistent with modified seawater compositions, and are close to the inferred isotopic compositions of ore-forming fluids from some other major VMS deposits (Costa *et al.* 1983, Barriga & Kerrich 1984, Munhá *et al.* 1986, MacLean & Hoy 1991, Huston *et al.* 1995). In contrast, in many other VMS deposits, the inferred values of the fluid are close to or even less than 0‰, reflecting more pristine seawater compositions. A different reaction-path is responsible for the isotopically heavy ore-forming fluids (Munhá *et al.* 1986), which affects fluid temperatures, scavenging of metals, and transport within the hydrothermal conduit.

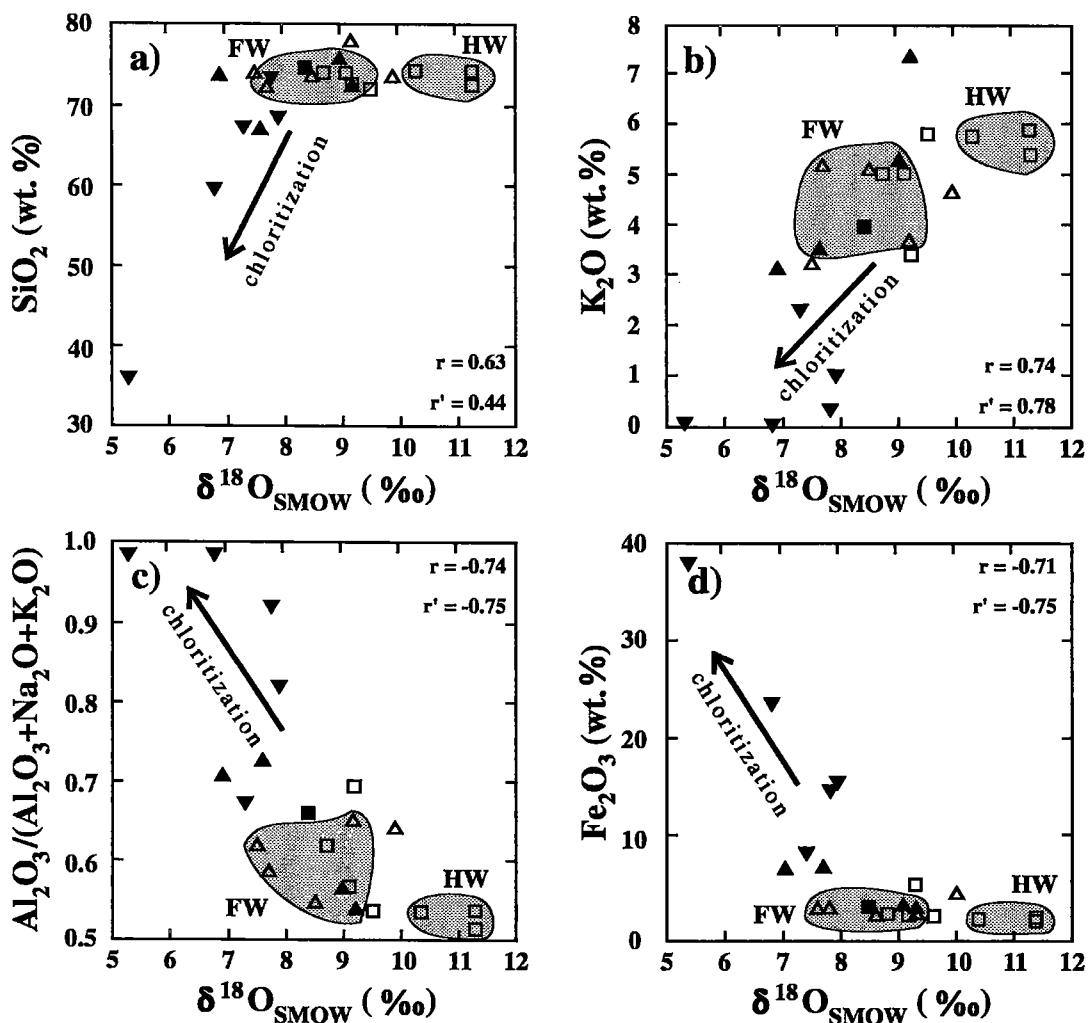


FIG. 26. Whole-rock SiO_2 , K_2O , $[\text{Al}_2\text{O}_3/(\text{Al}_2\text{O}_3 + \text{Na}_2\text{O} + \text{K}_2\text{O})]$, and Fe_2O_3 (total) versus $\delta^{18}\text{O}_{\text{SMOW}}$ of groundmass (open symbols) and whole-rock samples (filled symbols) (Table 3). r is the Pearson Product correlation coefficient, and r' is the Spearman's Rank correlation coefficient. Symbols as per Fig. 25.

HYDROTHERMAL ALTERATION

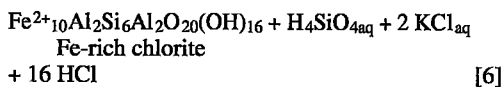
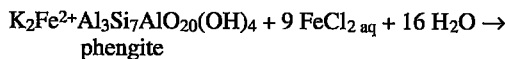
The least-altered samples of CT have irregular Na/K values and Mg contents that probably reflect post-depositional devitrification, also observed at Brunswick No. 12 (Lentz & Goodfellow 1993a). It is uncertain whether the chessboard albite and alkali feldspar represent primary phases or products of alteration (*cf.* Munhá *et al.* 1980). Both K-feldspar replacement of plagioclase and albitization of plagioclase have been observed in the outer (montmorillonite zone) around the Kuroko deposits (Green *et al.* 1983, and references therein), in the Iberian Pyrite Belt (Munhá *et al.* 1980), and some other massive sulfide deposits. Although the Na/K value

of infiltrating seawater can be expected to shift by exchange with the footwall sequence, albitization usually predominates in the Bathurst Camp, at least until, with increasing alteration, the pH of the altering fluid decreases to stabilize white mica and chlorite (*cf.* Lentz & Goodfellow 1993a).

The enrichment of Mg in the lower-footwall sedimentary rocks (distal) and occurrence of Mg-rich phengitic mica and Fe-rich clinocllore probably reflect relatively low-temperature conditions of formation ($<200^\circ\text{C}$), as a result of distal entrainment of seawater. The deposition of $\text{Mg}(\text{OH})_{2\text{aq}}$ in clays in felsic volcanic rocks has contributed to a pronounced decrease of the fluid's pH (Bischoff *et al.* 1981, Hajash & Chandler 1981, Shiraki *et al.* 1987).

Toward the proximal alteration zone at the Heath Steele B zone, there is an increase in chlorite abundance relative to white mica, as was also observed at Brunswick No. 12 (Lentz & Goodfellow 1993a). The chlorite compositions also become more Fe-rich toward the stockwork zone, as at Brunswick No. 12 (Juras 1981, Luff *et al.* 1992, Lentz & Goodfellow 1993a, 1996, and references therein) and Half Mile Lake, New Brunswick (Adair 1992, Lentz 1996b), as well as many other massive sulfide deposits (*e.g.*, Roberts & Reardon 1978, Hendry 1981, McLeod & Stanton 1984, Kranidiotis & MacLean 1987, Slack & Coad 1989, Leitch 1992). The chlorite in some deposits displays an Mg-enrichment trend (Urabe *et al.* 1983, Morton & Franklin 1987).

The chlorite-forming reaction at the expense of white mica is indicative of high Fe and Mg activities relative to K activity in the hydrothermal fluid, with the Fe end-member reaction given in equation 6.



This end-member reaction was formulated assuming Al immobility to illustrate the relative behavior of mobile components. The consumption of phengite occurs in an environment with a high activity of divalent metals and high temperature-dependent solubility of quartz. The general absence of free quartz in the chloritite implies SiO_2 leaching, although the fluid may be locally SiO_2 -saturated. However, chloritization may not necessarily always indicate leaching (eq. 7) at every stage of the alteration process:

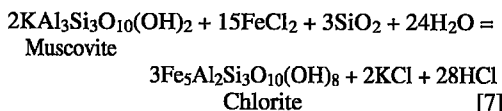


Figure 27 illustrates the possible reactions that form chlorite based on an $a\text{Na}^+/a\text{K}^+$ value equal to 10, typical of an ore-forming fluid originally dominated by seawater. The temperature of the probable end-member reaction for the more distal alteration should be less than 350°C (Fig. 27a) compared to the higher-temperature proximal stockwork alteration (350 to 400°C ; Fig. 27b). These reactions are near saturation with an aluminosilicate, on the basis of the Al-rich compositions of the chlorite. The stability of biotite is significantly reduced for the quartz-undersaturated equilibria; therefore, it would not have become a stable primary hydrothermal alteration phase in the stockwork, even if muscovite is present.

The inferred moderate- to high-temperature alteration trend at Heath Steele B zone is illustrated on Figure 27a

and b, respectively. The distal alteration zone (IV) generally contains ferroan clinocllore [$\text{Fe}/(\text{Fe} + \text{Mg})$ in the range 0.3–0.4, Fig. 27a], quartz and feldspar, and the highest component of phengite in the white mica. In the

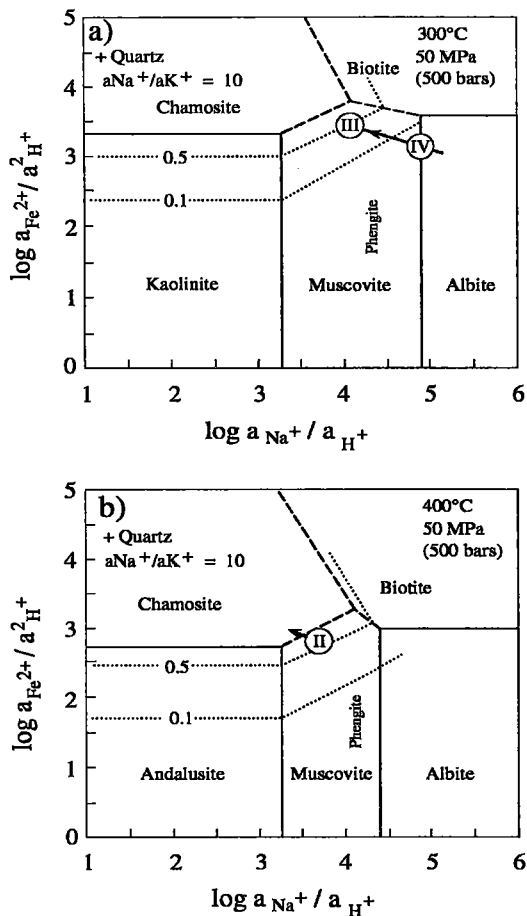


FIG. 27. $\log a(\text{Fe}^{2+})/a^2(\text{H}^+)$ versus $\log a(\text{Na}^+)/a(\text{H}^+)$ illustrating hypothetical conditions of hydrothermal alteration at 300°C (a) and 400°C (b) at 50 MPa (modified from Saccoccia & Seyfried 1994) for assemblages found in the most proximal (II), the intermediate (III), and the distal (IV) alteration zones observed in this section at the Heath Steele B zone. The stability fields of muscovite and annite were estimated for a fluid with an $a\text{Na}^+/a\text{K}^+$ of 10 (Bowers *et al.* 1984).

intermediate alteration zone (III), chlorite typically has an $\text{Fe}/(\text{Fe} + \text{Mg})$ value of 0.5 to 0.6, and feldspar is absent (Fig. 27a). The proximal alteration zones (II and I) are dominated by chamosite [$\text{Fe}/(\text{Fe} + \text{Mg}) > 0.7$]; quartz and muscovite are not always present (Fig. 27b). This trend indicates relatively high activity ratios for Fe/Mg, Fe/K, and Fe/Na in the discharging hydrothermal fluid. The increase in $\text{Fe}/(\text{Fe} + \text{Mg})$ content of chlorite

and phengitic mica toward the main hydrothermal conduit at Heath Steele B zone is indicative of high $a\text{Fe}^{2+}/a\text{Mg}^{2+}$ (cf. Shikazono & Kawahata 1987, Saccoccia & Seyfried 1994). For the mole fraction of chamosite (0.8) observed in the stockwork zone, the $\text{Fe}/\text{Mg}_{\text{fluid}}$ ratio is estimated to have been about 200 at 400°C, i.e., typical of the buoyant mineralizing fluid, whereas the $\text{Fe}/\text{Mg}_{\text{fluid}}$ approaches 0.5 for the distal alteration (at 300°C) for salinity conditions of normal seawater (Saccoccia & Seyfried 1994). In general, these estimates indicate marginal interaction of low-T shallowly circulating seawater with high-T modified seawater derived at depth (i.e., fluid mixing) or intermediate compositions of fluid obtained by altering Mg-rich (seawater-altered) rocks at the margins of the stockwork zone.

CONCLUSIONS

This whole-rock geochemical, mineral-chemical, and oxygen isotopic study describes geological and geochemical features of primary igneous and sedimentary rocks and the effects of hydrothermal alteration of those rocks hosting the Heath Steele B zone deposit. Overall, the principal results are:

- 1) Whole-rock composition of the footwall and hanging-wall CT packages are slightly but significantly different, on the basis of HFSE contents and ratios; they, therefore, do not represent the same unit.
- 2) Contents of immobile transition metals of the two footwall sedimentary packages are considerably different; the lower package petrographically and compositionally resembles rocks of the Miramichi Group, whereas the upper footwall sedimentary package, for the most part, resembles tuffaceous rocks of the Nepisiguit Falls Formation.
- 3) In the altered footwall, in particular the stockwork zone, there is an increase in the proportion of chlorite and sulfides, including pyrite and pyrrhotite, at the expense of groundmass components, feldspar and phyllosilicates, as the ore horizon is approached; these changes also are reflected in the whole-rock chemistry. The overall width of the recognizable altered zone is relatively small (~200 m), because it has been telescoped owing to extensive D_1 transposition. There is also a consistent increase in $(\text{Fe} + \text{Mg})/(\text{K} + \text{Na})$ and $\text{Al}_2\text{O}_3/(\text{Al}_2\text{O}_3 + \text{K}_2\text{O} + \text{Na}_2\text{O})$ toward the massive sulfides, which reflects the combined effects of alkali leaching and the increase in ratio of chlorite to white mica. These trends are coincident with an increase in whole-rock S, Cu, Co, As, and Sb, which reflects saturation in sulfides.
- 4) In this drill-hole section, the hanging-wall alteration is less than 50 m wide, with recognizably higher $(\text{Fe} + \text{Mg})/(\text{K} + \text{Na})$, Eu/Eu^* , Fe, Mn, Mg, S, and Ba, Co, Cu, Zn, Pb, Sb, and Hg, and lower $\text{Al}_2\text{O}_3/(\text{Al}_2\text{O}_3 + \text{K}_2\text{O} + \text{Na}_2\text{O})$ than rocks further up in the hanging-wall sequence.
- 5) The low Mn contents in the most-altered footwall rocks are indicative of low $f(\text{O}_2)$ conditions compared

to the underlying CT, which probably represents a distal feature considering the transposition involved. The higher Mn contents in the altered CT of the hanging wall are consistent with previous studies at Heath Steele.

6) The mineral assemblages and their relative proportions reflect primary and secondary litho-geochemical variations and upper greenschist-grade metamorphism. On the basis of selected mineral equilibria, these rocks reached approximately 450°C and 600 MPa during peak metamorphism, with the minerals generally showing an equilibrium distribution of major and trace elements.

7) Quartz phenocryst separates from the CT horizons in the footwall and hanging wall have slightly different $\delta^{18}\text{O}$ values. The whole-rock values for least-altered footwall and hanging wall are 7.5 to 9.5‰ and 10.3 to 11.3‰, respectively.

8) Whole-rock $\delta^{18}\text{O}$ values decrease with increased intensity of chloritic alteration toward the ore horizon. A sample of footwall chloritite has a $\delta^{18}\text{O}$ of 5.3‰; at the inferred temperature of formation (between 300 and 400°C), this value should approximate that of ore-forming fluid (~5 to 7‰), indicative of an extensively modified seawater composition. Whole-rock $\delta^{18}\text{O}$ values decrease from greater than 11‰ in the least-altered hanging wall to 8.7‰ in the alteration zone immediately above the ore.

9) Distal alteration in the footwall is manifested by chessboard albite, which variably replaces alkali feldspar phenocrysts. With increasing alteration (intermediate to proximal), the feldspar grains are progressively hydrolyzed to micas, and there is an increase in the $\text{Fe}/(\text{Fe} + \text{Mg})$ ratio and Al contents of the white mica (phengite – muscovite) and chlorite (ferroan clinocllore – magnesian chamosite). These changes reflect alkali and silica leaching at low pH and a high Fe/Mg in the fluid. For an estimated temperature of 400°C, chlorite compositions ($X_{\text{chamosite}} = 0.8$) near the stockwork indicates an $\text{Fe}/\text{Mg}_{\text{fluid}} \approx 200$ (modified seawater). At a lower inferred temperature (300°C), the chlorite ($X_{\text{chamosite}} = 0.3$) from the distal alteration indicates a major decrease in the Fe/Mg of the fluid, reflecting low-T, shallow infiltration of seawater into the peripheral environment of alteration.

10) Feldspar hydrolysis to Ba-bearing phengite and ferroan clinocllore in the immediate hanging-wall CT is indicative of continued venting of fluid through the CT and mixing with shallowly circulating Mg-rich seawater.

ACKNOWLEDGEMENTS

The authors thank the staff of Noranda Exploration Limited for the financial support and cooperation with this phase of the Heath Steele research project. Art Hamilton, chief geologist at Heath Steele Mines, helped familiarize the first author with the vast amount of information on the Heath Steele deposits. Discussions with Wayne Goodfellow (GSC), Chris Moreton (Noranda), and Reg Wilson (NBGSB) are greatly appreciated.

Comments on a preliminary version of the manuscript by Steven McCutcheon (NBGSB) were helpful. This manuscript benefitted from critical reviews by Drs. Timothy J. Barrett, Craig H.B. Leitch, and Robert F. Martin. This contribution forms part of the five-year, federal-provincial EXTECH II Agreement.

REFERENCES

- ADAIR, R.N. (1992): Stratigraphy, geochemistry, and structure of the Halfmile Lake Zn-Pb massive-sulfide deposit, New Brunswick. *Explor. Mining Geol.* **2**, 151-166.
- ANDERS, E. & EBIHARA, M. (1982): Solar-system abundances of the elements. *Geochim. Cosmochim. Acta* **46**, 2363-2380.
- BARRETT, T.J. & MACLEAN, W.H. (1991): Chemical, mass, and oxygen isotope changes during extreme hydrothermal alteration of an Archean rhyolite, Noranda, Quebec. *Econ. Geol.* **86**, 406-414.
- _____ & _____ (1994): Chemostratigraphy and hydrothermal alteration in exploration for VHMS deposits in greenstones and younger volcanic rocks. In *Alteration and Alteration Processes associated with Ore-forming Systems* (D.R. Lentz, ed.). *Geol. Assoc. Can., Short-Course Notes* **11**, 433-467.
- BARRIGA, F.J.A.S. & KERRICH, R. (1984): Extreme ^{18}O -enriched volcanics and ^{18}O -evolved marine water, Aljustrel, Iberian Pyrite Belt: transitions from high to low Rayleigh number convection regimes. *Geochim. Cosmochim. Acta* **48**, 1021-1031.
- BATTEY, M.H. (1955): Alkali metasomatism and the petrology of some keratophyres. *Geol. Mag.* **92**, 104-126.
- BAYLISS, P. (1975): Nomenclature of the trioctahedral chlorites. *Can. Mineral.* **13**, 178-180.
- BISCHOFF, J.L., RADTKE, A.S. & ROSENBAUER, R.J. (1981): Hydrothermal alteration of graywacke by brine and seawater. Roles of alteration and chloride complexing on metal solubilization at 200° and 350°C. *Econ. Geol.* **76**, 659-676.
- BOWERS, T.S., JACKSON, K.J. & HELGESON, H.C. (1984): *Equilibrium Activity Diagrams for Coexisting Minerals and Aqueous Solutions at Pressures and Temperatures to 5 kb and 600°C*. Springer-Verlag, Berlin, Germany.
- BRYNDZIA, L.T. & SCOTT, S.D. (1987): The composition of chlorite as a function of sulfur and oxygen fugacity: an experimental study. *Am. J. Sci.* **287**, 50-76.
- BUCHER-NURMINEN, K. (1987): A recalibration of the chlorite-biotite-muscovite geobarometer. *Contrib. Mineral. Petrol.* **96**, 519-522.
- CAMERON, B.I., HANNINGTON, M.D., BRISBIN, D.I. & KOOPMAN, E.R. (1993): Preliminary mineral chemical studies of phyllosilicates in host rocks of the Kidd Creek massive sulphide deposit, Timmins, Ontario. *Geol. Surv. Can., Pap.* **93-1E**, 157-164.
- CHEN, T.T. & PETRUK, W. (1980): Mineralogy and characteristics that affect recoveries of metals and trace-elements from the ore at Heath Steele Mines, New Brunswick. *Can. Inst. Mining Metall., Bull.* **73**(823), 167-179.
- CLAYTON, R.N. & MAYEDA, T.K. (1963): The use of bromine pentafluoride in the extraction of oxygen from oxides and silicates for isotopic analysis. *Geochim. Cosmochim. Acta* **27**, 43-52.
- COSTA, U.R., BARNETT, R.L., & KERRICH, R. (1983): The Mattagami Lake Mine Archean Zn-Cu sulfide deposit, Quebec: hydrothermal coprecipitation of talc and sulfides in a sea-floor brine pool - evidence from geochemistry, $^{18}\text{O}/^{16}\text{O}$, and mineral chemistry. *Econ. Geol.* **78**, 1144-1203.
- CRAIG, H. (1961): Standard for reporting concentrations of deuterium and oxygen-18 in natural waters. *Science* **133**, 1833-1834.
- DAHL, P.S., WEHN, D.C. & FELDMANN, S.G. (1993): The systematics of trace-element partitioning between coexisting muscovite and biotite in metamorphic rocks from the Black Hills, South Dakota, USA. *Geochim. Cosmochim. Acta* **57**, 2487-2505.
- DAVIES, J.F., GRANT, R.W.E. & WHITEHEAD, R.E.S. (1979): Immobile trace elements and Archean volcanic stratigraphy in the Timmins mining area, Ontario. *Can. J. Earth. Sci.* **16**, 305-311.
- _____ & WHITEHEAD, R.E.S. (1980): Further immobile data from altered volcanic rocks, Timmins mining area, Ontario. *Can. J. Earth. Sci.* **17**, 419-423.
- DECHOW, E. (1960): Geology, sulfur isotopes and origin of the Heath Steele ore deposits, Newcastle, N.B., Canada. *Econ. Geol.* **55**, 539-556.
- DE ROO, J.A., MORETON, C., WILLIAMS, P.F. & VAN STAAL, C.R. (1990): The structure of the Heath Steele region, Bathurst Camp, New Brunswick. *Atl. Geol.* **26**, 27-41.
- _____, WILLIAMS, P.F. & MORETON, C. (1991): Structure and evolution of the Heath Steele base metal sulfide orebodies, Bathurst Camp, New Brunswick, Canada. *Econ. Geol.* **86**, 927-943.
- _____, _____ & _____ (1992): Structure and evolution of the Heath Steele base metal sulfide orebodies, Bathurst Camp, New Brunswick, Canada - a reply. *Econ. Geol.* **87**, 1687-1688.
- DOSTAL, J. & STRONG, D.F. (1983): Trace-element mobility during low-grade metamorphism and silicification of basaltic rocks from Saint John, New Brunswick. *Can. J. Earth. Sci.* **20**, 431-435.
- FYFFE, L.R. (1995): Regional geology and litho-geochemistry, in the vicinity of the Chester VMS deposit, Big Bald Mountain area, New Brunswick, Canada. *Explor. Mining Geol.* **4**, 153-173.
- GOODFELLOW, W.D. (1975): Major and minor element halos in the volcanic rocks at Brunswick No. 12 sulphide deposit, N.B., Canada. In *Developments in Economic Geology* **1**,

- Geochemical Exploration 1974 (L.L. Elliot & W.K. Fletcher, eds.). Elsevier, Amsterdam, The Netherlands (279-295).
- _____ & WAHL, J.L. (1976): Water extracts of volcanic rocks – detection of anomalous halos at Brunswick No. 12 and Heath Steele B-Zone massive sulphide deposits. *J. Geochem. Explor.* **6**, 35-59.
- GREEN, G.R., OHMOTO, H., DATE, J. & TAKAHASHI, T. (1983): Whole-rock oxygen isotope distribution in the Fukazawa-Kosaka area, Hokuroko district, Japan, and its potential application to mineral exploration. In *The Kuroko and Related Volcanogenic Massive Sulfide Deposits* (H. Ohmoto & B.J. Skinner, eds.). *Econ. Geol., Monogr.* **5**, 395-411.
- GUIDOTTI, C.V. (1984): Micas in metamorphic rocks. In *Micas* (S.W. Bailey, ed.). *Rev. Mineral.* **13**, 357-467.
- HAJASH, A. & CHANDLER, G.W. (1981): An experimental investigation of high-temperature interactions between seawater and rhyolite, andesite, basalt and peridotite. *Contrib. Mineral. Petrol.* **78**, 240-254.
- HAMILTON, A., PARK, A. & MORETON, C. (1993): Geology of Heath Steele Mines, Bathurst Camp, New Brunswick. In *Guidebook to the Metallogeny of the Bathurst Camp* (S.R. McCutcheon & D.R. Lentz, eds.). *Third Annual CIM Field Trip Conf.*, 50-65.
- HEINRICH, C.A. & EADINGTON, P.J. (1986): Thermodynamic predictions of the hydrothermal chemistry of arsenic, and their significance for the paragenetic sequence of some cassiterite – arsenopyrite – base metal sulfide deposits. *Econ. Geol.* **81**, 511-529.
- HENDRY, D.A.F. (1981): Chlorites, phengites, and siderites from the Prince Lyell ore deposits, Tasmania, and the origin of the deposit. *Econ. Geol.* **76**, 285-303.
- HOY, L.D. (1993): Regional evolution of hydrothermal fluids in the Noranda District, Quebec: evidence from $\delta^{18}\text{O}$ values from volcanogenic massive sulfide deposits. *Econ. Geol.* **88**, 1526-1541.
- HUGHES, C.J. (1973): Spillites, keratophyres, and the igneous spectrum. *Geol. Mag.* **109**, 513-527.
- HUSTON, D.L., TAYLOR, B.E., BLEEKER, W., STEWART, B., COOK, R. & KOOPMAN, E.R. (1995): Isotope mapping around the Kidd Creek deposit, Ontario: application to exploration and comparison with other geochemical indicators. *Explor. Mining Geol.* **4**, 175-185.
- _____, _____ & WATANABE, D.H. (1996): Productivity of volcanic-hosted massive sulfide districts: new constraints from the $\delta^{18}\text{O}$ of quartz phenocrysts in cogenetic felsic rocks. *Geology* **24**, 459-462.
- JAMBOR, J.L. (1979): Mineralogical evaluation of proximal–distal features in New Brunswick massive-sulfide deposits. *Can. Mineral.* **17**, 649-664.
- JURAS, S.J. (1981): *Alteration and Sulphide Mineralization in Footwall Felsic and Sedimentary Rocks, Brunswick No. 12 Deposit, Bathurst, New Brunswick, Canada*. M.Sc. thesis, Univ. New Brunswick, Fredericton, New Brunswick.
- KAWACHI, Y., GRAPES, R.H., COOMBS, D.S. & DOWSE, M. (1983): Mineralogy and petrology of a piemontite-bearing schist, western Otago, New Zealand. *J. Metamorphic Geol.* **1**, 353-372.
- KRANDIOTIS, P. & MACLEAN, W.H. (1987): Systematics of chlorite alteration at the Phelps Dodge massive sulfide deposit, Matagami, Quebec. *Econ. Geol.* **82**, 1898-1911.
- KRETZ, R. (1961): Some applications of thermodynamics to coexisting minerals of variable composition. Examples: orthopyroxene – clinopyroxene and orthopyroxene – garnet. *J. Geol.* **69**, 361-387.
- _____ (1993): A garnet population in Yellowknife schist, Canada. *J. Metamorphic Geol.* **11**, 101-120.
- LAIRD, J. (1988): Chlorites: metamorphic petrology. In *Hydrous Phyllosilicates* (S.W. Bailey, ed.). *Rev. Mineral.* **19**, 405-453.
- LANGTON, J.P. & MCCUTCHEON, S.R. (1993): Brunswick Project, NTS 21 P/5 West, 21 P/4 West Gloucester County, New Brunswick. In *Current Research* (S.A. Abbott, ed.). *New Brunswick Dep. Natural Resources and Energy, Mineral Resources Inf. Circ.* **93-1**, 31-51.
- LEAT, P.T., JACKSON, S.E., THORPE, R.S. & STILLMAN, C.J. (1986): Geochemistry of bimodal basalt–subalkaline/peralkaline rhyolite provinces within the southern British Caledonides. *J. Geol. Soc. London* **143**, 259-273.
- LE BAS, M.J., LEMAITRE, R.W., STRECKEISEN, A. & ZANNETTIN, B. (1986): A chemical classification of volcanic rocks based on the total alkali–silica diagram. *J. Petrol.* **27**, 745-750.
- LEITCH, C.H.B. (1992): Mineral chemistry of selected silicates, carbonates, and sulphides in the Sullivan and North Star stratiform Zn–Pb deposits, British Columbia, and in district-scale altered and unaltered sediments. *Geol. Surv. Can., Pap.* **92-1E**, 83-93.
- _____ & LENTZ, D.R. (1994): The Gresens approach to mass balance constraints of alteration systems: methods, pitfalls, examples. In *Alteration and Alteration Processes Associated with Ore-Forming Systems* (D.R. Lentz, ed.). *Geol. Assoc. Can., Short-Course Notes* **11**, 161-192.
- LENTZ, D.R. (1994): Exchange reactions applied to hydrothermally altered rocks with examples from biotite-bearing assemblages. In *Alteration and Alteration Processes Associated with Ore-Forming Systems* (D.R. Lentz, ed.). *Geol. Assoc. Can., Short-Course Notes* **11**, 69-99.
- _____ (1995a): Preliminary evaluation of six in-house rock geochemical standards from the Bathurst camp, New Brunswick. In *Current Research 1994* (S.A.A. Merlino, ed.). *New Brunswick Dep. Natural Resources and Energy, Minerals and Energy Div., Misc. Rep.* **18**, 81-89.
- _____ (1995b): Stratigraphy and structure of the Key Anacon massive-sulphide deposits compared with the Brunswick deposits, Bathurst Mining Camp, New Brunswick. In *Geoscience Research 1994* (J.P. Langton, ed.). *New Brunswick Dep. Natural Resources and Energy, Minerals and Energy Div., Misc. Rep.* **15**, 23-44.

- _____ (1996a): Trace-element systematics of felsic volcanic rocks associated with massive-sulphide deposits in the Bathurst Mining Camp: petrogenetic, tectonic and chemostratigraphic implications for VMS deposits. In Trace Element Geochemistry of Volcanic Rocks: Applications for Massive Sulphide Exploration (D.A. Wyman, ed.). *Geol. Assoc. Can., Short-Course Notes* **12**, 359-402.
- _____ (1996b): Recent advances in lithogeochemical exploration for massive-sulphide deposits in volcano-sedimentary environments: petrogenetic, chemostratigraphic, and alteration aspects with examples from the Bathurst Camp, New Brunswick. In Current Research 1995 (B.M.W. Carroll, ed.). *New Brunswick Dep. Natural Resources and Energy, Minerals and Energy Div., Mineral Resources Rep.* **96-1**, 73-119.
- _____ (1997): Re-analysis of a section through the Heath Steele B-B5 zone area, Bathurst Mining Camp, New Brunswick: exploration implications. In Current Research 1996 (B.M.W. Carroll, ed.). *New Brunswick Dep. Natural Resources and Energy, Minerals and Energy Div., Mineral Resource Rep.* **97-4**, 113-127.
- _____ & GOODFELLOW, W.D. (1992a): Re-evaluation of the petrology and depositional environment of felsic volcanic and related rocks in the vicinity of the Brunswick No. 12 massive sulphide deposit, Bathurst Mining Camp, New Brunswick. *Geol. Surv. Can., Pap.* **92-1E**, 333-342.
- _____ & _____ (1992b): Re-evaluation of the petrochemistry of felsic volcanic and volcanoclastic rocks near the Brunswick No. 6 and 12 massive sulphide deposits, Bathurst Mining Camp, New Brunswick. *Geol. Surv. Can., Pap.* **92-1E**, 343-350.
- _____ & _____ (1993a): Petrology and mass-balance constraints on the origin of quartz augen schist associated with the Brunswick massive sulfide deposits, Bathurst, New Brunswick. *Can. Mineral.* **31**, 877-903.
- _____ & _____ (1993b): Mineralogy and petrology of the stringer sulphide zone in the Discovery Hole at the Brunswick No. 12 massive sulphide deposit, Bathurst, New Brunswick. *Geol. Surv. Can., Pap.* **93-1E**, 249-258.
- _____ & _____ (1993c): Geochemistry of the stringer sulphide zone in the Discovery Hole at the Brunswick No. 12 massive sulphide deposit, Bathurst, New Brunswick. *Geol. Surv. Can., Pap.* **93-1E**, 259-269.
- _____ & _____ (1994a): Petrology and geochemistry of altered volcanic and sedimentary rocks associated with the FAB stringer sulphide zone, Bathurst, New Brunswick. *Geol. Surv. Can., Pap.* **94-D**, 123-133.
- _____ & _____ (1994b): Character, distribution, and origin of zoned hydrothermal alteration features at the Brunswick No. 12 massive sulphide deposit, Bathurst Mining Camp, New Brunswick. In Current Research (S.A. Abbott, ed.). *New Brunswick Dep. Natural Resources and Energy, Minerals Resources, Inf. Circ.* **94-1**, 94-119.
- _____ & _____ (1996): Intense silicification of footwall sedimentary rocks in the stockwork alteration zone beneath the Brunswick No. 12 massive sulphide deposit, Bathurst, New Brunswick. *Can. J. Earth Sci.* **33**, 284-302.
- _____, _____ & BROOKS, E. (1996): Chemostratigraphy and depositional environment of an Ordovician sedimentary section across the Miramichi Group - Tetagouche Group contact, northeastern New Brunswick. *Atl. Geol.* **32**, 101-122.
- _____ & VAN STAAL, C.R. (1995): Predeformational origin of massive sulfide mineralization and associated footwall alteration at the Brunswick No. 12 deposit, Bathurst, New Brunswick: evidence from the zoned porphyry dike. *Econ. Geol.* **90**, 453-463.
- _____ & WILSON, R.A. (1997): Chemostratigraphic analysis of the volcanic and sedimentary rocks in the Heath Steele B-B5 zone area, Bathurst Camp, New Brunswick: stratigraphic and structural implications. *Geol. Surv. Can., Pap.* **97-D**, 21-33.
- LEWCZUK, L. (1990): Microprobe analyses of phyllosilicates, Bathurst Camp. *New Brunswick Research and Productivity Council, Rep.* **90-10**.
- LUFF, W., GOODFELLOW, W.D. & JURAS, S.J. (1992): Evidence for a feeder pipe and associated alteration at the Brunswick No. 12 massive sulfide deposit. *Explor. Mining Geol.* **1**, 167-185.
- LUSK, J. (1969): Base metal zoning in the Heath Steele B-1 orebody, New Brunswick, Canada. *Econ. Geol.* **64**, 509-518.
- _____ (1992): Structure and evolution of the Heath Steele base metal sulfide orebodies, Bathurst Camp, New Brunswick, Canada - a discussion. *Econ. Geol.* **87**, 1682-1687.
- MACLEAN, W.H. (1990): Mass change calculations in altered rock series. *Mineral. Deposita* **25**, 44-49.
- _____ & BARRETT, T.J. (1993): Lithogeochemical techniques using immobile elements. *J. Geochem. Explor.* **48**, 109-133.
- _____ & HOY, L.D. (1991): Geochemistry of hydrothermally altered rocks at the Horne mine, Noranda, Quebec. *Econ. Geol.* **86**, 506-528.
- MASSONNE, H.-J. & SCHREYER, W. (1987): Phengite geobarometry based on the limiting assemblage with K-feldspar, phlogopite, and quartz. *Contrib. Mineral. Petrol.* **96**, 212-224.
- MCBRIDE, D.E. (1976): *Geology of Heath Steele Mines, New Brunswick*. Ph.D. thesis, Univ. New Brunswick, Fredericton, New Brunswick.
- McCUTCHEON, S.R. (1992): Base-metal deposits of the Bathurst-Newcastle district: characteristics and depositional models. *Explor. Mining Geol.* **1**, 105-119.
- _____, LANGTON, J.P., VAN STAAL, C.R. & LENTZ, D.R. (1993): Stratigraphy, tectonic setting and massive-sulphide deposits of the Bathurst Mining Camp, northern New Brunswick. In Guidebook to the Metallogeny of the Bathurst Camp (S.R.

- McCutcheon & D.R. Lentz, eds.). *Trip 4, Bathurst'93 Third Annual CIM Geological Field Conf.*, 1-39.
- McDONALD, D.W.A. (1984): *Fragmental Pyrrhotite Ore at Heath Steele Mines, New Brunswick*. M.Sc. thesis, Univ. New Brunswick, Fredericton, New Brunswick.
- McLEOD, R.L. & STANTON, R.L. (1984): Phyllosilicates and associated minerals in some Paleozoic stratiform sulfide deposits of southeastern Australia. *Econ. Geol.* **79**, 1-22.
- MCMILLIAN, R.N. (1969): *A Comparison of Geological Environments of the Base Metal Sulphide Deposits of the B-Zone and North Boundary Zone at Heath Steele Mines, New Brunswick*. M.Sc. thesis, Univ. Western Ontario, London, Ontario.
- MONIER, G. & ROBERT, J.-L. (1986): Muscovite solid solutions in the system $K_2O-MgO-FeO-Al_2O_3-SiO_2-H_2O$: an experimental study at 2 kbar PH_2O and comparison with natural Li-free white micas. *Mineral. Mag.* **50**, 257-266.
- MORETON, C. (1994): *The Stratigraphy, Structure, and Geometry of the B, B-5 and E Zones, Heath Steele Mines, Newcastle, New Brunswick*. Ph.D. thesis, Univ. New Brunswick, Fredericton, New Brunswick.
- _____ & WILLIAMS, P.F. (1986): Structural and stratigraphic relationships at the B-Zone orebody, Heath Steele Mines, Newcastle, New Brunswick. *Geol. Surv. Can., Pap.* **86-1B**, 57-64.
- MORTON, R.L. & FRANKLIN, J.M. (1987): Two-fold classification of Archean volcanic-associated massive sulfide deposits. *Econ. Geol.* **82**, 1057-1063.
- MOTIL, M.J. (1983): Metabasalts, axial hot springs, and the structure of the hydrothermal systems at mid-ocean ridges. *Geol. Soc. Am., Bull.* **94**, 161-180.
- MUNHÁ, J., BARRIGA, F.J.A.S. & KERRICH, R. (1986): High ^{18}O ore-forming fluids in volcanic-hosted base metal massive sulfide deposits: geologic, $^{18}O/^{16}O$, and D/H evidence from the Iberian Pyrite Belt; Crandon, Wisconsin; and Blue Hill, Maine. *Econ. Geol.* **81**, 530-552.
- _____, FYFE, W.S. & KERRICH, R. (1980): Adularia, the characteristic mineral of felsic spilites. *Contrib. Mineral. Petrol.* **75**, 15-19.
- NELSON, G.A. (1983): *Alteration of Footwall Rocks at Brunswick No.6 and Austin Brook Deposits, Bathurst, New Brunswick, Canada*. M.Sc. thesis, Univ. New Brunswick, Fredericton, New Brunswick.
- O'NEIL, J.R., SHAW, S.E. & FLOOD, R.H. (1977): Oxygen and hydrogen isotope compositions as indicators of granite genesis in the New England Batholith, Australia. *Contrib. Mineral. Petrol.* **62**, 313-328.
- OWSIAKI, L. (1980): *The Geology of the C-Zone, Heath Steele Mine, New Brunswick*. M.Sc. thesis, Univ. New Brunswick, Fredericton, New Brunswick.
- PEARCE, J.A., HARRIS, N.B.W. & TINDLE, A.G. (1984): Trace element discrimination diagrams for the tectonic interpretation of granitic rocks. *J. Petrol.* **25**, 956-983.
- POWELL, R. & EVANS, J.A. (1983): A new geobarometer for the assemblage biotite - muscovite - chlorite - quartz. *J. Metamorphic Geol.* **1**, 331-336.
- RAMBALDI, E.R. (1973): Variation in the composition of muscovite and biotite in some metamorphic rocks near Bancroft, Ontario. *Can. J. Earth Sci.* **10**, 869-880.
- REFAAT, A.M. & ABDALLAH, Z.M. (1979): Geochemical study of coexisting biotite and chlorite from Zaker granitic rocks of Zanjan area, northwest Iran. *Neues Jahrb. Mineral., Abh.* **136**, 262-275.
- RIVERIN, G. & HODGSON, C.J. (1980): Wall-rock alteration at the Millenbach Cu-Zn Mine, Noranda, Quebec. *Econ. Geol.* **75**, 424-444.
- ROBERTS, R.G. & REARDON, E.J. (1978): Alteration and ore-forming processes at Mattagami Lake Mine, Quebec. *Can. J. Earth Sci.* **15**, 1-21.
- SACCOCCIA, P.J. & SEYFRIED, W.E., JR. (1994): The solubility of chlorite solid solutions in 3.2 wt% NaCl fluids from 300-400°C, 500 bars. *Geochim. Cosmochim. Acta* **58**, 567-585.
- SCHMIDT, J.M. (1988): Mineral and whole-rock compositions of seawater-dominated hydrothermal alteration at the Arctic volcanogenic massive sulfide prospect, Alaska. *Econ. Geol.* **83**, 822-842.
- SHIKAZONO, N. & KAWAHATA, H. (1987): Compositional differences in chlorite from hydrothermally altered rocks and hydrothermal ore deposits. *Can. Mineral.* **25**, 465-474.
- SHIRAKI, R., SAKAI, H., ENDOH, M. & KISHIMA, N. (1987): Experimental studies on rhyolite- and andesite-seawater interactions at 300°C and 1000 bars. *Geochem. J.* **21**, 139-148.
- SKINNER, R. (1974): Geology of the Tetagouche Lakes, Bathurst and Nepisiguit Falls map-areas, New Brunswick. *Geol. Surv. Can., Mem.* **371**.
- SLACK, J.F. & COAD, P.R. (1989): Multiple hydrothermal and metamorphic events in the Kidd Creek volcanogenic massive sulfide deposit, Timmins, Ontario: evidence from tourmalines and chlorites. *Can. J. Earth Sci.* **26**, 694-715.
- STARKEY, J. (1959): Chess-board albite from New Brunswick, Canada. *Geol. Mag.* **96**, 141-145.
- SUTHERLAND, J.K. (1967): Chlorites of the Anaconda-Caribou deposit, New Brunswick. *New Brunswick Res. Productivity Council, Res. Note* **8**.
- _____, & HALLS, C. (1969): Composition of some New Brunswick sphalerites. *New Brunswick Res. Productivity Council, Res. Note* **21**.
- SVERJENSKY, D.A. (1985): The distribution of divalent trace elements between sulfides, oxides, silicates, and hydrothermal solutions. I. Thermodynamic basis. *Geochim. Cosmochim. Acta* **49**, 853-864.

- SYMMES, G.H. & FERRY, J.M. (1992): The effect of whole-rock MnO content on the stability of garnet in pelitic schists during metamorphism. *J. Metamorphic Geol.* **10**, 221-237.
- TAYLOR, H.P., JR. (1968): The oxygen isotope geochemistry of igneous rocks. *Contrib. Mineral. Petrol.* **19**, 1-71.
- _____ (1980): The effects of assimilation of country rocks by magmas on $^{18}\text{O}/^{16}\text{O}$ and $^{87}\text{Sr}/^{86}\text{Sr}$ systematics in igneous rocks. *Earth Planet. Sci. Lett.* **47**, 243-254.
- TAYLOR, S.R. & McLENNAN, S.M. (1985): *The Continental Crust: its Composition and Evolution*. Blackwell Scientific Publications, Boston, Massachusetts.
- TOULMIN, P., III, BARTON, P.B., JR. & WIGGINS, L.B. (1991): Commentary on the sphalerite geobarometer. *Am. Mineral.* **76**, 1038-1051.
- URABE, T., SCOTT, S.D. & HATTORI, K. (1983): A comparison of footwall-rock alteration and geothermal systems beneath some Japanese and Canadian volcanogenic massive sulfide deposits. In *The Kuroko and Related Volcanogenic Massive Sulfide Deposits* (H. Ohmoto & B.J. Skinner, eds.). *Econ. Geol., Monogr.* **5**, 345-364.
- VAN STAAL, C.R. (1987): Tectonic setting of the Tetagouche Group in northern New Brunswick: implications for plate tectonic models in the northern Appalachians. *Can. J. Earth. Sci.* **24**, 1329-1351.
- _____ & FYFFE, L.R. (1991): Dunnage and Gander Zones, New Brunswick: Canadian Appalachian Region. *New Brunswick Dep. Natural Resources and Energy, Mineral Resources, Geosci. Rep.* **91-2**.
- _____, _____, LANGTON, J.P. & McCUTCHEON, S.R. (1992): The Ordovician Tetagouche Group, Bathurst Camp, northern New Brunswick, Canada: history, tectonic setting and distribution of massive sulfide deposits. *Explor. Mining Geol.* **1**, 93-103.
- WAHL, J. (1978): *Distribution of Major-, Minor-, and Trace-Elements in Rocks Around Heath Steele and Key Anaconda Mines, New Brunswick*. Ph.D. thesis, Univ. New Brunswick, Fredericton, New Brunswick.
- WENNER, D.B. & TAYLOR, H.P., JR. (1971): Temperatures of serpentinization of ultramafic rocks based on $\text{O}^{18}/\text{O}^{16}$ fractionation between coexisting serpentine and magnetite. *Contrib. Mineral. Petrol.* **32**, 165-185.
- WHALEN, J.B., CURRIE, K.L. & CHAPPELL, B.W. (1987): A-type granites: geochemical characteristics, discrimination and petrogenesis. *Contrib. Mineral. Petrol.* **95**, 407-419.
- WHITEHEAD, R.E.S. (1973): Environment of stratiform sulphide deposition; variation in Mn/Fe ratio in host rocks at Heath Steele Mine, New Brunswick, Canada. *Mineral. Deposita* **8**, 148-160.
- _____ & GOVETT, G.J.S. (1974): Exploration rock geochemistry – detection of trace element halos at Heath Steele Mines (N.B., Canada) by discriminant analysis. *J. Geochem. Explor.* **3**, 371-386.
- WILSON, R.A. (1993): Geology of the Heath Steele – Halfmile Lakes area; Northumberland County, New Brunswick. *New Brunswick Dep. Natural Resources and Energy, Mineral Resources Div., Rep. Invest.* **25**.
- WINCHESTER, J.A. & FLOYD, P.A. (1977): Geochemical discrimination of different magma series and their differentiation products using immobile elements. *Chem. Geol.* **20**, 325-343.
- WOOD, S.A., CRERAR, D.A. & BORCSIK, M.P. (1987): Solubility of the assemblage pyrite – pyrrhotite – magnetite – sphalerite – galena – gold – stibnite – bismuthinite – argentite – molybdenite in H_2O – NaCl – CO_2 solutions from 200° to 350°C. *Econ. Geol.* **82**, 1864-1887.

Received May 14, 1996, revised manuscript accepted March 6, 1997.

Note added in proof: Further follow-up research (Lentz 1997) and exploration (Art Hamilton, pers. commun.) in the Heath Steele B–B5 area has shown that the exhalative Heath Steele horizon seems to be structurally repeated by folding on the south limb of the overturned, doubly plunging, isoclinal F_{1B} fold (see Fig. 2), as implied by the stratigraphic and structural revisions proposed in this study and by Lentz & Wilson (1997). Furthermore, the contact between the Heath Steele belt and the Flat Landing Brook rhyolites (Fig. 2) is probably a late D_1 thrust, as indicated by de Roo *et al.* (1990) and Moreton (1994), in contrast to a locally faulted (Heath Steele Fault), conformable relationship as shown here (Lentz 1997).